CLNS-82/522
January, 1982

Hadronic Wave Functions in QCD†

G. Peter Lepage
Nuclear Studies, Newman Laboratory
Cornell University, Ithaca, NY 14853

[Written with collaboration from

S. J. Brodsky
Stanford Linear Accelerator Center, Stanford, CA

T. Huang
Institute of High Energy Physics, Beijing, China

P. B. Mackenzie
Fermi National Accelerator Laboratory, Batavia, IL]

† Invited talk presented at the Banff Summer Institute on Particle Physics, Banff, Alberta, Canada, August, 1981.

1. INTRODUCTION

It is now widely believed that hadrons are composites built of quarks and gluons whose interactions are governed by quantum chromodynamics (QCD). The nature of this internal structure is the key to an understanding of hadronic properties, both at short and long distances. However the connection between the hadrons and their constituents often seems vague in applications of perturbative QCD. If we are to push beyond perturbation theory, we require a conceptual framework within which these notions can be made precise. A particularly convenient and intuitive framework is based upon the Fock state decomposition of hadronic states which arises naturally in the 'light-cone quantization' of QCD. In this approach, a hadron is characterized by a set of Fock state wave functions, the probability amplitudes for finding different combinations of bare quarks and gluons in the hadron at a given 'light-cone time' $\tau = t + z$. These wave functions provide the essential link between hadronic phenomena at short distances (perturbative) and at long distances (non-perturbative).

The use of light-cone quantization and equal τ wave functions, rather than the more familiar equal t wave functions, is necessary for a sensible Fock state expansion. In light-cone quantization, the Fock state vacuum is an eigenstate of the full light-cone Hamiltonian ($H_{LC} \equiv P^- = P^0 - P^3$, conjugate to τ). Consequently all of the bare quanta in an hadronic Fock state are associated with the hadron; none are disconnected elements of the vacuum (Fig. 1). It is also convenient to use τ-ordered light-cone perturbation theory (LCPTh), in place of

covariant perturbation theory, for much of the analysis of light-cone dominated processes such as deep inelastic scattering, or large-$p_\perp$ exclusive reactions. Light-cone quantization and perturbation theory are briefly reviewed in Appendix A.

In these lectures, we explore the properties of the Fock state wave functions, and their relation to measurable quantities.[1,2] In Section 2, we describe the Fock state basis and wave functions in greater detail. We examine general properties of the wave functions, and the implications of the renormalization group in this context. We also discuss briefly a number of processes — $\pi^+ \to \mu\nu$, $\pi^0 \to \gamma\gamma$, deep inelastic scattering,... — using this language.

In Section 3 we review the analysis of exclusive processes involving transfer of large momenta.[3] This includes a derivation of the basic formulae and a discussion of the complications due to end-point and pinch singularities. Large $p_\perp$ exclusive processes provide one of the best tools for probing the valence wavefunctions of hadrons, as well as an important testing ground for perturbative QCD.

Finally in Section 4 we discuss bound states of heavy quarks (ψ,Υ,...). These mesons are unique in that we have considerable understanding of their internal structure, largely due to the apparent predominance of the $Q\bar{Q}$ Fock state. We examine the reasons for this, and discuss the ways in which we can exploit this understanding to study both non-perturbative and perturbative features of QCD. As a footnote to this section, we also discuss in Appendix B the significance of perturbative expansions in QCD focusing on the choice of definition for α_s. We propose a new

procedure which provides a natural criterion for the convergence of such expansions.

2. The Fock State Description of Hadrons

A. Definitions

At any given light-cone time $\tau = t + z$, we can define a set of basis states (Appendix A)

$$\begin{aligned} &|0\rangle \\ &|q\bar{q}\colon \underline{k}_i, \lambda_i\rangle = b^+(\underline{k}_1\lambda_1)d^+(\underline{k}_2\lambda_2)|0\rangle \\ &\quad\vdots \end{aligned} \tag{2.1}$$

where $b^+, d^+, \ldots$ are the Fourier transforms of the unrenormalized field operators at time τ, and where $\underline{k}_i = (k^+ \equiv (k^0 - k^3), \vec{k}_\perp)_i$ is the three-momentum of the i^{th} parton and λ_i its helicity. Here k^+ is always positive, and the Fock states are normalized such that $\langle \underline{k}|\underline{q}\rangle = 2k^+(2\pi)^3\delta^3(\underline{k} - \underline{q})$. Of course the elements, other than the vacuum, of this Fock state basis are not eigenstates of the full Hamiltonian $H_{LC}(= P^-)$. However they form a useful basis for studying the physical states of the theory. A pion, for example, is described by a state

$$|\pi\rangle = \sum_{q\bar{q}} |q\bar{q}\rangle\, \psi_{q\bar{q}/\pi} + \sum_{q\bar{q}g} |q\bar{q}g\rangle\, \psi_{q\bar{q}g/\pi} + \ldots \tag{2.2a}$$

or to be more precise, for a pion with momentum $\underline{P} = (P^+, P_\perp)(\Rightarrow P^- = (P_\perp^2 + M_\pi^2)/P^+)$,

$$|\pi\colon P^+, P_\perp\rangle = \sum_{n,\lambda_i} \int \tilde{\prod_i} \frac{dx_i d^2k_{\perp i}}{\sqrt{x_i}\ 16\pi^3}\ |n\colon x_i P^+, x_i P_\perp + k_{\perp i}, \lambda_i\rangle\, \psi_{n/\pi}(x_i, k_{\perp i}, \lambda_i) \tag{2.2b}$$

where the sum is over all Fock states and helicities, and where

$$\tilde{\prod_i} dx_i \equiv \prod_i dx_i \; \delta(1 - \sum_i x_i)$$
$$\tilde{\prod_i} d^2k_{\perp i} = \prod_i d^2k_{\perp i} \; 16\pi^3 \delta^2(\sum_j k_{\perp j}) \tag{2.3}$$

enforce three-momentum conservation. Notice that wave function $\psi_{n/\pi}(x_i, k_{\perp i}, \lambda_i)$, the amplitude for finding bare partons with momenta $(x_i P^+, x_i P_\perp + k_{\perp i})$, is independent of the pion's momentum. This special feature of equal τ wave functions is not surprising since x_i, the longitudinal momentum fraction carried by the parton $(0 \leq x_i \leq 1)$, and k_i, its momentum 'transverse' to the pion's direction of motion, are frame independent quantities.

Throughout this analysis, we employ the physical light-cone gauge, $\eta \cdot A = A^+ = 0$, for the gluon field. Use of such gauges results in well known simplifications in the perturbative analysis of light-cone dominated processes. Furthermore, they are indispensible if one desires a simple, intuitive Fock space, for there are neither negative norm gauge boson states nor ghost states in $A^+ = 0$ gauge. Thus each term in the normalization condition

$$\sum_{n \, \lambda_i} \int \tilde{\prod_i} \frac{dx_i d^2k_{\perp i}}{16\pi^3} \left|\psi_{n/\pi}(x_i, k_{\perp i}, \lambda_i)\right|^2 = 1 \tag{2.4}$$

(which follows from $\langle \pi:\underline{P} | \pi:\underline{P}' \rangle = 2P^+(2\pi)^3 \delta^3(\underline{P} - \underline{P}')$) is positive.

Any hadron state, such as $|\pi\rangle$, must be an eigenstate of the Hamiltonian. Consequently, when working in a frame in which $\underline{P}_\pi = (1, 0)$

and $P_\pi^- = M_\pi^2$, the state $|\pi\rangle$ satisfies an equation

$$(M_\pi^2 - H_{LC})\ |\pi\rangle = 0$$

Projecting this onto the various Fock states $\langle q\bar{q}|$, $\langle q\bar{q}g|$, ... results in an infinite number of coupled integral (eigenvalue) equations

$$\left[M^2 - \sum_i \left(\frac{k^2+m^2}{x}\right)_i\right] \begin{bmatrix} \psi_{q\bar{q}} \\ \psi_{q\bar{q}g} \\ \vdots \end{bmatrix} \quad \begin{bmatrix} \langle q\bar{q}|V|q\bar{q}\rangle\langle q\bar{q}|V|q\bar{q}g\rangle\ldots \\ \langle q\bar{q}g|V|q\bar{q}\rangle\ \ldots \\ \vdots \end{bmatrix} \begin{bmatrix} \psi_{q\bar{q}} \\ \psi_{q\bar{q}g} \\ \vdots \end{bmatrix} \qquad (2.5)$$

where V is the interaction part of H_{LC}. Diagrammatically, V involves completely inducible interactions — i.e. diagrams having no internal propagators — coupling the Fock states (Fig. 2). In principle these equations determine the hadronic spectrum and wave functions.

The bulk of the probability in a non-relativistic system, such as positronium or the Υ, is in a single Fock state — here in $|e\bar{e}\rangle$ and $|b\bar{b}\rangle$ respectively. In such systems one obtains a single equation for the dominant wave function by tracing over the remaining Fock states. Thus, for positronium, we have (Fig. 3)[4]

$$\left(M^2 - \frac{k_\perp^2+m_e^2}{x(1-x)}\right) \psi_{e\bar{e}}(x,k_\perp) = \int_0^1 dy \int_0^\infty \frac{d^2\ell_\perp}{16\pi^3} V_{eff}(x,k_\perp;y,\ell_\perp;M^2)\psi_{e\bar{e}}(y,\ell_\perp). \qquad (2.6)$$

The effects of all higher Fock states are included in V_{eff}, the sum of all two-particle irreducible interaction kernels — i.e. diagrams having no internal two-particle propagators (Fig.3b). The effective potential, $V_{eff} \sim V_{Coulomb}$, is little modified by higher Fock states, so this

procedure and others closely related to it (e.g. Bethe-Salpeter equation) are well warranted. However, higher Fock states are most likely quite important for a light-quark hadron, and consequently V_{eff} cannot help but be very complex in this case. In particular, retardation effects must then become significant, as is evident from the normalization condition for the valence Fock state wave function:

$$\sum_{\lambda_i}\int\tilde{\prod_i}\frac{dx_i d^2k_{\perp i}}{16\pi^3}\,|\psi_v(x_i,k_{\perp i},\lambda_i)|^2 = 1 - \langle\psi_v^*\left|\frac{\partial V_{eff}}{\partial M^2}\right|\psi_v\rangle \leq 1 \tag{2.7}$$

– the expectation of $\partial V_{eff}/\partial M^2$ equals the possibility of higher (i.e. non-valence) Fock states. So one is forced to consider the full coupled channel problem (Eq.(2.5)) when analyzing hadrons. Traditional two-body (or three-body) bound state formalisms seem inappropriate in highly relativistic, strong coupling theories.

B. General Properties of Fock State Wave Functions

One major advantage of the Fock state description of a hadron is that much intuition exists about the behavior of bound state wave functions. So, while the task of solving Eq.(2.5) for QCD remains formidable, there is nevertheless much we can say about the hadronic wave functions. An important feature that is immediately evident from Eq.(2.5) is that all wave functions have the general form

$$\psi_n(x_i,k_{\perp i},\lambda_i) = \frac{1}{M^2 - \sum_i\left[\frac{k_\perp^2+m^2}{x}\right]_i}\,(V\psi) \tag{2.8}$$

Consequently ψ_n tends to vanish when

$$\varepsilon = M^2 - \sum_i \left(\frac{k_\perp^2 + m^2}{x} \right)_i \to -\infty \qquad (2.9)$$

This is intuitively plausible. In The Fock state expansion, we think of the bare quanta as being on mass shell —

$$\text{i.e.} \quad k_i^- = \frac{k_{\perp i}^2 + m_i^2}{x_i} \implies k_i^2 = m_i^2$$

—but off (light-cone) energy shell. Parameter ε measures how far off energy shell a Fock state is, and thus we see that a physical particle has little probability of being in a Fock state far off shell. In general ε is large when $k_{\perp i}^2$ or m_i^2 is large, or x_i small — i.e. the wave function should vanish as $k_{\perp i}^2, m_i^2 \to \infty$ or $x_i \to 0$.

Formally these constraints appear as boundary conditions on the wave functions, and are related to self-adjointness of the Hamiltonian. Notice for example that the expectation value of the free Hamiltonian, $\sum_i \left(\frac{k_\perp^2 + m^2}{x} \right)_i$, is finite only if

$$\begin{aligned} k_{\perp i}^2 \, \psi_n(x_i, k_{\perp i}, \lambda_i) &\to 0 \quad \text{as } k_i^2 \to \infty \\ \psi_n(x_i, k_{\perp i}, \lambda_i) &\to 0 \quad \text{as } x_i \to 0 \end{aligned} \qquad (2.10)$$

As we shall see in the next section, neither of these constraints is satisfied in perturbative QCD unless we introduce ultraviolet ($k_\perp \to \infty$) and infrared ($x \to 0$) regulators.

A further source of intuition about wave functions is provided by the physics of non-relativistic bound states ($\langle v \rangle \ll c$). In the rest frame ($P^+ = P^- = M$, $P_\perp = 0$), equal time (t) and equal light-cone time ($\tau = t + z/c$) are almost identical for a non-relativistic system since the speed of light is effectively infinite. Consequently the usual (equal time) Schrödinger wave function should be almost the same as the light-cone wave function. To make this connection, notice that the i^{th} constituent has longitudinal momentum

$$k_i^+ = x_i M = k_i^0 + k_i^3$$
$$\simeq m_i + O(m_i v^2) + k_i^3$$

where the energy k_i^0 is just the mass plus small corrections, due to kinetic and potential energy, of $O(m_i v^2) \ll k_i^3 \sim O(m_i v)$. Thus if we write

$$x_i = \frac{m_i}{M} + \tilde{x}_i \quad ,$$

$\tilde{x}_i M$ is essentially equal to k_i^3 for the parton, and a Schrödinger wave function is then converted to a light-cone wave function simply by replacing $k_i^3 \to \tilde{x}_i M$. This is also evident when it is noted that all energy denominators have the form

$$M^2 - \sum_i \left(\frac{k_\perp^2 + m^2}{x} \right)_i \simeq 2M \left\{ E_{N.R.} - \sum_i \left(\frac{k_\perp^2 + (\tilde{x}M)^2}{2m} \right)_i \right\}$$

when $\tilde{x}_i \ll x_i$. Consequently one expects non-relativistic wave functions to be strongly peaked at

$$x_i = \frac{m_i}{M} \qquad k_{\perp i} = 0$$

with $k_{\perp i}$, $\tilde{x}_i M \ll m_i$, in the same way Schrödinger wave functions are peaked at low $\vec{k}_i$ ($\ll m_i$). This is well illustrated by the wave function for ground state positronium or hydrogen (valid for $k_\perp^2, (x_e M - m_e)^2 \ll m_e^2$):

$$\psi(x_e, k_\perp) \simeq \left(\frac{2M\gamma^3}{\pi}\right)^{\frac{1}{2}} \frac{8\pi\gamma}{(k_\perp^2 + (x_e M - m_e)^2 + \gamma^2)^2} \tag{2.11}$$

where $\gamma = \alpha m_R$, and m_R is the reduced mass. Such reasoning has immediate implications for hadron physics. For example, the charmed quark in a D meson tends to carry most of the meson's longitudinal momentum ($x_c \sim m_c/M_D \sim 1$), and therefore fragementation functions should be broader (in z) for D mesons than for π mesons.

C. Renormalization; Truncated Fock Space [5]

The basic ansatz of perturbative QCD is that the short distance behavior of the theory is perturbative; only perturbative interactions are sufficiently singular to contribute at short distances. Consequently wave functions behave in much the same way as perturbative amplitudes in LCPTh when $k_{\perp i}^2 \to \infty$ (see Section 3). Such a comparison (Fig. 4) indicates, for example, that $\psi_{q\bar{q}} \sim 1/k_\perp^2$ and $\psi_{q\bar{q}g} \sim 1/k_\perp$ for $k_\perp$ large. This behavior violates boundary conditions (2.10), and leads to infinities in the unitarity sum (2.4), energy expectation values, and in the wave functions themselves. Of course this is not unexpected, given that the wave functions and the theory are as yet unrenormalized.

To make the theory finite, we truncate the Fock space by in effect discarding all Fock states with light-cone energy (Eq.(2.9)) $|\varepsilon| \gtrsim \Lambda^2$.

This ultraviolet cut-off can be introduced by using Pauli-Villars and related regulators, so as to preserve Poincaré invariance and gauge invariance.[6] The end result is that all internal loop integrations are finite, and the wave functions become well behaved for $k_\perp^2 \gtrsim \Lambda^2$ — e.g., $\psi_{q\bar{q}} \sim 1/k_\perp^4$ and $\psi_{q\bar{q}g} \sim 1/k_\perp^3$ for $k_\perp^2 >> \Lambda^2$.

Usually one takes $\Lambda \to \infty$ when computing. However the key physical characteristic of renormalizable theories is that this cut-off has no effect on the results for any process provided only that Λ is much larger than all mass scales, energies, and so on relevant to the process of interest. Fock states with $|\varepsilon| \gtrsim \Lambda^2$ need never be explicitly included; all low-energy effects due to them can be absorbed into the coupling constants, masses, etc. appearing in an effective Lagrangian (or Hamiltonian) for the truncated theory — e.g.

$$\mathcal{L}^{(\Lambda)} = \bar{\psi}(i\not{\partial} - g(\Lambda)\not{A} - m(\Lambda))\psi - \tfrac{1}{4}F^2 + O(\tfrac{1}{\Lambda}\bar{\psi}\sigma\cdot F\psi + \ldots)$$

These bare parameters vary with Λ in the usual way, as more or less of the high energy Fock states are absorbed:

$$\Lambda^2 \frac{d}{d\Lambda^2}\alpha_s(\Lambda) = \beta(\alpha_s(\Lambda), \frac{m(\Lambda)}{\Lambda})$$
$$\vdots$$

In general, non-renormalizable interactions appear as well, but these are suppressed by powers of $1/\Lambda$, as is evident from simple dimensional arguments. Notice also that the effective Lagrangian can change radically as Λ passes thresholds for new heavy quarks, or say for quark substructure.

The bare parameters — $g(\Lambda)$, $m(\Lambda)$, ... — are the effective couplings

and masses of the theory at energies of order Λ (i.e. distances $\sim 1/\Lambda$). Indeed, as we shall see, a process or quantity in which only a single scale Q is relevant is most naturally expressed in terms of the couplings, masses, wave functions, etc. of the theory with cut-off $\Lambda \sim Q$. Of course one must compute with $\Lambda >> Q$, but the dominant effect of vertex and self-energy corrections is to replace $g(\Lambda)$, $m(\Lambda)$, $\psi^{(\Lambda)}$... by $g(Q)$, $m(Q)$, $\psi^{(Q)}$... Thus as Q is increased, ever finer structure is unveiled in the wave functions and in the theory. Also we are always dealing with a finite cut-off, so that couplings, masses, and in particular wave functions are both well defined and well behaved.

The dependence of the wave functions $\psi^{(\Lambda)}(x_i, k_{\perp i}, \lambda_i)$ on Λ for fixed x_i and $k_{\perp i}$ $(k_{\perp i}^2 << \Lambda^2)$ is multiplicative:

$$\psi_n^{(\Lambda)}(x_i, k_{\perp i}, \lambda_i) = \prod_j \left[\frac{Z_j^{(\Lambda)}}{Z_j^{(\Lambda_o)}}\right]^{\frac{1}{2}} \psi_n^{(\Lambda_o)}(x_i, k_{\perp i}, \lambda_i) \qquad (2.12)$$

where $Z_j^{(\Lambda)}$ is the usual wave function renormalization constant for the j^{th} parton. This formula is easily understood by recalling that $Z_j^{(\Lambda)}$ is the probability of finding a 'bare' parton in a 'dressed' parton. Also it follows that $0 \leq Z_j^{(\Lambda)} \leq 1$. Furthermore, $Z_j^{(\Lambda)}$ generally decreases with increasing Λ since the effective phase space, and therefore the probability, for the multi-parton Fock states in a dressed parton increases with Λ. Although the probability shifts from Fock state to Fock state with varying Λ, the total probability is always conserved:

$$\sum_{n,\lambda_i} \int \tilde{\Pi}_i \frac{dx_i d^2k_{\perp i}}{16\pi^3} \left|\psi_n^{(\Lambda)}(x_i,k_{\perp i},\lambda_i)\right|^2 = 1 + 0\left(\frac{m^2}{\Lambda^2}\right)$$

One final modification of the theory is required. The polarization sum for gluons in $A^+ = 0$ gauge is singular as $k^+ = x \to 0$:

$$\sum_{\lambda} \epsilon_\mu(\underline{k},\lambda)\epsilon_\nu^*(\underline{k},\lambda) = -g_{\mu\nu} + \frac{\eta_\mu k_\nu + \eta_\nu k_\mu}{x} \tag{2.13}$$

where $\underline{k} = (x,k_\perp)$ and $k^- = k_\perp^2/x$. As a result, wave functions for states with gluons diverge as $x_{gluon} \to 0$, again contrary to the boundary conditions (2.10). However the singularity in (2.13) is to some extent an artifact of light-cone gauge. It is properly regulated by replacing [7]

$$\frac{1}{x^n} \to \frac{1}{2}\left\{\frac{1}{(x+i\delta)^n} + \frac{1}{(x-i\delta)^n}\right\} \tag{2.14}$$

Physical amplitudes or cross sections are independent of δ provided it is sufficiently small, which implies that gluons decouple when $x_{gluon} \lesssim \delta$ for some small δ. Thus in effect the wave function does vanish as $x_{gluon} \to 0$; we can use regulator (2.14), with a small but non-zero δ, to remove gluons with $x \lesssim \delta$ from the wave function. Typically the cut-off point must be $\delta \lesssim \langle k_\perp \rangle / Q$ where $\langle k_\perp \rangle$ is some average of the gluon's $k_\perp$, and Q is the momentum scale of the probe. So as Q increases, so does the number of 'wee' gluons. Notice finally that $\langle k_\perp \rangle$ can never vanish, since very long wavelength gluons cannot couple to a color singlet wave function. Thus, with finite δ and Λ cut-offs, all Fock state wave functions are well behaved both as $x_i \to 0$ and as $k_{\perp i} \to \infty$.

D. Calculating

In principle, the hadronic wave functions determine all of the properties of a hadron. Here we illustrate the relation between the wave functions and measurable quantities by briefly examining a number of processes, particularly for pions. These examples also demonstrate the calculational rules for using wave functions — i.e. an amplitude involving Fock state ψ_n, describing a hadron with $\underline{P} = (P^+, P_\perp)$, has the form

$$\sum_{\lambda_i} \int \tilde{\prod_i} \frac{dx_i d^2k_{\perp i}}{\sqrt{x_i}\, 16\pi^3} \; \psi_n(x_i, k_{\perp i}, \lambda_i) \;\; T_n(x_i P^+, x_i P_\perp + k_{\perp i}, \lambda_i) \qquad (2.15)$$

where T_n is the irreducible scattering amplitude with the hadron replaced by Fock state n. If only the valence wave function is to be used, T_n is irreducible with respect to the valance Fock state only (e.g. no reducible $q\bar{q}$ propagators for π); while otherwise contributions from all Fock states must be summed, and T_n is completely irreducible.

$\pi \to \mu\nu$

The leptonic width of the $\pi^\pm$ is one of the simplest of all processes because it involves only the $q\bar{q}$ Fock state. The sole contribution is from

$$\langle 0 | \bar{\psi}_u \gamma^+ \frac{1-\gamma_5}{\sqrt{2}} \psi_d | \pi \rangle = -P^+ f_\pi$$

$$= \int \frac{dx d^2k_\perp}{16\pi^3} \psi^{(\Lambda)}_{q\bar{q}}(x, k_\perp) \frac{\sqrt{n_c}}{\sqrt{2}} \left\{ \frac{\bar{v}_\downarrow}{\sqrt{1-x}} \gamma^+ \frac{1-\gamma_5}{\sqrt{2}} \frac{u_\uparrow}{\sqrt{x}} - (\uparrow \leftrightarrow \downarrow) \right\}$$

where $n_c = 3$ is the number of colors, and $f_\pi \simeq 93$ MeV. Thus we

have

$$\int_0^1 dx \int \frac{d^2k_\perp}{16\pi^3} \psi_{q\bar{q}}^{(\Lambda)}(x,k_\perp) = \frac{f_\pi}{2\sqrt{3}} \tag{2.16}$$

This result must be independent of cut-off Λ up to corrections of order λ^2/Λ^2, where λ is some typical hadronic scale ($\lesssim$ 1 GeV). Eq.(2.16) is an important constraint on the normalization of the $q\bar{q}$ wave function, indicating among other things that there is a finite probability for finding a pure $q\bar{q}$ state in the pion.

π Form Factor

An exact expression for the pion's electromagnetic form factor is (Fig. 5)[8]

$$F_\pi(q_\perp^2) = \sum_{n,\lambda_i} \sum_q e_q \int \prod_i \frac{dx_i d^2\tilde{k}_{\perp i}}{16\pi^3} \psi_n^{(\Lambda)*}(x_i,\tilde{k}_{\perp i},\lambda_i)\psi_n^{(\Lambda)}(x_i,k_{\perp i},\lambda_i) \qquad \Lambda^2 >> q_\perp^2 \tag{2.17a}$$

where e_q is the charge of the struck quark and where

$$\tilde{k}_{\perp i} = \begin{cases} k_{\perp i} - x_i q_\perp + q_\perp & \text{for the struck quark} \\ k_{\perp i} - x_i q_\perp & \text{for all other partons} \end{cases} \tag{2.17b}$$

As in Eq.(2.2b), the transverse momenta $\tilde{k}_{\perp i}$ appearing as arguments in ψ^* correspond not to the full transverse momenta of the partons, but rather to the full $k_\perp$ minus $x_i q_\perp$, to account for the motion of the pion. In the limit $q_\perp \to 0$ (i.e. $\tilde{k}_\perp \to k_\perp$), the right hand side of (2.17a) becomes identical to the unitarity sum (Eq.(2.4), and therefore $F_\pi(0) = 1$. The form factor at large $q_\perp$ is discussed at length in Section 3.

Deep Inelastic Scattering ($\gamma^*\pi \to \overline{X}$)

To leading order in $\alpha_s(Q)$, the pion's structure functions are determined by the τ-ordered diagrams in Fig.6a. Furthermore, only the region $m^2 \ll k_\perp^2 \ll Q^2(1-x)$ contributes to this order ($Q^2 = q_\perp^2$). This has two important consequences: first, we can neglect $k_\perp$ relative to $q_\perp$ to leading order; and second, we can set the ultraviolet cut-off $\Lambda \sim Q$ since only Fock states with $k_\perp^2 \ll Q^2$ are important (again to leading order only). The structure functions are then

$$2MF_1(x,Q) \simeq \frac{F_2(x,Q)}{x} \simeq \sum_a e_a^2 \, G_{a/\pi}(x,Q) \tag{2.18a}$$

where, from Fig. 6a,

$$G_{a/\pi}(x,Q) \equiv \sum_{n,\lambda_i} \int \tilde{\prod_i} \frac{dx_i d^2k_{\perp i}}{16\pi^3} \left|\psi_{n/\pi}^{(Q)}(x_i,k_{\perp i},\lambda_i)\right|^2 \sum_{b=a} \delta(x_b - x) \tag{2.18b}$$

is the number (density) of partons of type a with longitudinal momentum fraction x (the $\sum_b$ is over all partons of type a in Fock state n). Eq.(2.18b) leads immediately to a very simple interpretation of the structure function moments:

$$\int_0^1 dx \, x^{n+1} \, G_{a/\pi}(x,Q) = \frac{\langle \pi | \overline{\psi}_a(0)\gamma^+(i\overleftrightarrow{D}^+)^{n+1}\psi_a(0)|\pi\rangle^{(Q)}}{(2P_\pi^+)^{n+2}} \tag{2.19}$$

where the matrix element is evaluated with ultraviolet cut-off $\Lambda = Q$, and where $D^+ = \partial^+$ in light-cone gauge. Thus the Q dependence of the moments is determined by the cut-off dependence of (twist-two) local operators.

Relation (2.18a) is corrected in $O(\alpha_s(Q))$ and beyond by diagrams such as that in Fig. 6b, which contributes only when $\ell_\perp \sim Q$ (in $A^+ = 0$ gauge). Diagrams like that in Fig. 6c are suppressed by powers of $1/Q^2$ due to the

additional hard propagators absent in the leading terms.

Although all Fock states contribute to the structure functions, it is likely that the valence state dominates near $x = 1$. This region involves Fock states far off-shell: $\langle\varepsilon\rangle \sim -\frac{\langle k_\perp^2 + m^2\rangle}{1-x} \to -\infty$ as $x \to 1$ (cf Eq.2.9). If perturbative interactions dominate here, the $x \sim 1$ behavior of the wave function is approximated by that of the simplest connected interaction kernel (Fig.7), just as for the large $k_\perp$ behavior. This implies (for an arbitrary hadron H)[8]

$$G_{q/H}^{pert} \sim (1-x)^{2n_s - 1 + |\Delta|} \quad \text{as } x \to 1 \tag{2.20}$$

where n_s is the number of spectator partons (= 1,2 for mesons, baryons) and Δ is the difference between the struck quark's helicity and that of the hadron (and where QCD evolution has not been included). Clearly the valence state, for which n_s is smallest, is most important as $x \to 1$.

The $(1-x)^3$ behavior suggested by Eq.(2.20) for protons is consistent with experiment, and there is some evidence for the helicity dependence predicted. Unfortunately, however, the situation is complicated by non-perturbative contributions, which could well be important down to very small 1-x. Any non-perturbative wave function which is a strongly peaked function of $\varepsilon = M^2 - \sum_i \left(\frac{k_\perp^2 + m^2}{x}\right)_i$ gives (Eq.(2.18b))[9]

$$G_{q/H}^{non\text{-}pert} \sim (1-x)^{2n_s - 1} \; F(\varepsilon_{min}) \qquad \text{as } x \to 1 \tag{2.21}$$

with $\varepsilon_{min} \sim -\frac{m^2}{1-x}$. Since F vanishes quickly as $\varepsilon_{min} \sim -\frac{m^2}{1-x} \to -\infty$, the perturbative effects (Eq.2.20) ultimately dominate. However, to the extent

that quark masses are negligible (i.e. for $1-x>>m^2/\langle k_\perp^2\rangle$), this ansatz, at least, gives important non-perturbative corrections.

$\underline{\pi^0 \to \gamma\gamma}$

The $\gamma^*\pi^0\to\gamma$ vertex (Fig.8) can be parameterized in terms of the $\pi^0-\gamma$ transition form factor $F_{\pi\gamma}(Q^2=-q^2)$:

$$\Gamma_{\mu\nu} = + ie^2 F_{\pi\gamma}(Q^2)\varepsilon_{\mu\nu\rho\sigma}p^\rho q^\sigma$$

The techniques of Section 3, when applied to $F_{\pi\gamma}$, show that only the $q\bar{q}$ Fock state is relevant as $Q^2\to\infty$.[11] Surprisingly, this is also the case for very low $Q^2\sim 0(m_\pi^2)$, given that m_π is much smaller than the typical momentum scale, λ, governing pionic wave functions. This allows us to relate the $\pi^0\to\gamma\gamma$ decay rate,

$$\Gamma_{\pi^0\to\gamma\gamma} = \frac{\alpha^2\pi}{4} m_\pi^3 F_{\pi\gamma}^2(0) \ ,$$

directly to the $q\bar{q}$ wave function of the pion.

There are two basic types of contribution to $F_{\pi\gamma}(0)$, as illustrated in Fig. 9. The first (Fig.9a) involves the direct annihilation of the $q\bar{q}$ into two photons:[12]

$$F_{\pi\gamma}^{(a)}(Q^2) = \frac{\Gamma^{+i}_{(a)}\varepsilon^i_\perp}{ie^2(\varepsilon_\perp x q_\perp)} \qquad (\varepsilon_\perp\cdot q_\perp = 0)$$

$$= -2\sqrt{n_c}\,(e_u^2-e_d^2)\int_0^1 dx \int\frac{d^2k_\perp}{16\pi^3}\psi_{q\bar{q}}^{(\Lambda)}(x,k_\perp)\,\frac{1}{Z_2^{(\Lambda)}}$$

$$\cdot\left\{\frac{\varepsilon_\perp x(q_\perp(1-x)+k_\perp)}{(\varepsilon_\perp x q_\perp)(q_\perp(1-x)+k_\perp)^2} + \begin{bmatrix} x\leftrightarrow(1-x) \\ k_\perp\leftrightarrow -k_\perp \end{bmatrix}\right\} \qquad (2.22)$$

$$\to -\frac{\sqrt{n_c}(e_u^2-e_d^2)}{8\pi^2}\int_0^1 dx\,\frac{\psi_{q\bar{q}}^{(\Lambda)}(x,0_\perp)}{Z_2^{(\Lambda)}} \quad \text{as } Q^2=q^2\to 0$$

where the $Z_2^{(\Lambda)}$ is due to vertex and propagator renormalizations, and $\Lambda >> \lambda$.

The second contribution has one photon coupling 'inside' the pion's wave function — i.e. strong interactions occur between the photon interactions (Fig.9b). We can treat this photon as an external field which is approximately constant throughout the pion's volume, since the photon's wavelength ($\sim 1/m_\pi$) is assumed to be much larger than the pion radius ($\sim 1/\lambda$). Now a fermion propagator in a constant external field is modified only by a phase:

$$\begin{aligned} S_A(x-y) &= \langle y| \frac{1}{\not p - e\not A - m} |x\rangle \\ &= \langle y| e^{-eA\cdot\frac{\partial}{\partial p}} \frac{1}{\not p - m} |x\rangle \\ &= e^{-ie(y-x)\cdot A} S_F(x-y). \end{aligned}$$

Consequently the $q\bar{q}$ wave function for a pion in this field is modified by a phase $e^{-iey\cdot A}$ where y is the $q\bar{q}$ separation. To avoid double counting Fig. 9a, this phase is applied to the truncated wave function (i.e. without an external $q\bar{q}$ propagator),

$$\Gamma_T(x,K_\perp) = \frac{\not p \gamma_5}{\sqrt{2}} \psi^{(\Lambda)}_{q\bar{q}}(x,k_\perp) ,$$

and furthermore only the first order term is required for Fig. 8b — i.e.

$$e^{-iey\cdot A}\ \Gamma_T \to -\frac{\not p \gamma_5}{\sqrt{2}}\, e\frac{\partial}{\partial k_\mu}\, \psi^{(\Lambda)}_{q\bar{q}}(x,k_\perp).$$

where $ie\varepsilon\cdot A \to e\frac{\partial}{\partial k_\mu}$ in momentum space, and $q_\perp \to 0$ is assumed. Thus the second contribution becomes (Fig. 10)

$$F^{(b)}_{\pi\gamma}(Q^2) = -\frac{\varepsilon^i_\perp \Gamma^{i+}_{(b)}}{ie^2(\varepsilon_\perp x q_\perp)}$$

$$\simeq -\frac{\sqrt{n_c}(e_u^2-e_d^2)}{2i(\varepsilon_\perp x q_\perp)}\int dx\,\frac{d^2k_\perp}{16\pi^3}\{\varepsilon_\perp\cdot\frac{\partial}{\partial k_\perp}\psi^{(\Lambda)}_{q\bar{q}}(x,k_\perp)\}\frac{1}{Z_2^{(\Lambda)}}\,\frac{x(1-x)}{-k_\perp^2}$$

$$\cdot\left\{\frac{\bar{v}_\downarrow}{\sqrt{1-x}}\gamma^+\frac{u_\uparrow}{\sqrt{x}}\;\frac{\bar{u}_\uparrow(x,\tfrac{1}{2}q_\perp+k_\perp)}{\sqrt{x}}\not{p}\gamma_5\;\frac{v_\downarrow(1-x,\tfrac{1}{2}q_\perp-k_\perp)}{\sqrt{1-x}}+(\uparrow\leftrightarrow\downarrow)\right\}$$

$$\simeq \frac{\sqrt{n_c}(e_u^2-e_d^2)}{8\pi^3}\int dx\,\frac{d^2k_\perp}{k_\perp^2}\{\varepsilon_\perp\cdot\frac{\partial}{\partial k_\perp}\psi^{(\Lambda)}_{q\bar{q}}(x,k_\perp)\}\frac{k_\perp x q_\perp}{\varepsilon_\perp x q_\perp}\frac{1}{Z_2^{(\Lambda)}}$$

as $q_\perp \to 0$. The angular integral is easily done, giving

$$F^{(b)}_{\pi\gamma}(0) \simeq \frac{\sqrt{n_c}(e_u^2-e_d^2)}{8\pi^2}\int_0^1 dx\int_0^\infty dk_\perp^2\,\frac{\partial}{\partial k_\perp^2}\psi^{(\Lambda)}_{q\bar{q}}(x,k_\perp)\frac{1}{Z_2^{(\Lambda)}} = \mp F^{(a)}_{\pi\gamma}(0)$$

Thus the complete $\pi\gamma$ form factor at $Q=0$ is

$$F_{\pi\gamma}(0) = -\frac{\sqrt{n_c}(e_u^2-e_d^2)}{4\pi^2}\int_0^1 dx\,\frac{\psi^{(\Lambda)}_{q\bar{q}}(x,0_\perp)}{Z_2^{(\Lambda)}} + O\left(\frac{m_\pi^2}{\lambda^2}\right)$$

The data for $\pi^0\to\gamma\gamma$ is well fit by the PCAC prediction[13]

$$F_{\pi\gamma}(0) = -\frac{1}{4\pi^2}\,n_c(e_u^2-e_d^2)\,\frac{1}{f_\pi}$$

and so we have yet another constraint on the $q\bar{q}$ wave function for a pion:

$$\int_0^1 dx\,\frac{\psi^{(\Lambda)}_{q\bar{q}}(x,0_\perp)}{Z_2^{(\Lambda)}} \simeq \frac{\sqrt{n_c}}{f_\pi} = \frac{\sqrt{3}}{f_\pi} \qquad (2.23)$$

Constraints such as Eqs.(2.16) and (2.23) are important in the phenomenological construction of hadronic wave functions. For example, a simple ansatz for the pion's non-perturbative valence wave function is

$$\psi^{(\Lambda)}_{q\bar{q}}(x,k_\perp) \simeq A\, e^{-b^2 k_\perp^2/x(1-x)}$$

where $\Lambda \sim$ a GeV. Eqs.(2.16) and (2.23) then imply

$$A = \frac{\sqrt{3}}{f_\pi}\, Z_2^{(\Lambda)} \qquad b^2 = \frac{1}{(4\pi f_\pi)^2}\, Z_2^{(\Lambda)}$$

From Eq.(2.4), we can compute the probability of finding a pion in its valence state for this ansatz;

$$P_{q\bar{q}/\pi} = \frac{Z_2^{(\Lambda)}}{4} \leq \frac{1}{4} \ ,$$

while from Eq.(2.17) we can calculate the 'radius' of the valence state:[14]

$$(R_{q\bar{q}/\pi})^2 = 18b^2 = Z_2^{(\Lambda)}\ 13\ \text{GeV}^{-2}$$

If the valence state is comparable in size to the pion, the probability $Z_2^{(\Lambda)}$ of finding a bare quark in a dressed quark must be near one, from this equation, and in that case $P_{q\bar{q}/\pi} \sim 1/4$. One could (and should) go on to study the $x \sim 1$ behavior of the π structure function, the form factor at large Q^2, etc. with this ansatz, and with others. In this way one hopes to develop a deeper understanding of the detailed structure of hadrons.

3. EXCLUSIVE PROCESSES IN QCD

A. Introduction

In this section we review the analysis of exclusive processes with large momentum transfer. Generally one finds that such an amplitude factors into a convolution of quark distribution amplitudes $\phi(x_i,Q)$, one for each hadron, with a hard scattering amplitude T_H. The pion's electromagnetic form factor, for example, can be written as[1,3]

$$F_\pi(Q^2) = \int_0^1 dx \int_0^1 dy\ \phi_\pi^*(x,Q)\ T_H(x,y,Q)\ \phi_\pi(y,Q)\left(1+O\left(\frac{1}{Q^2}\right)\right) \qquad (3.1)$$

Here T_H is the scattering amplitude but with the pions replaced by collinear $q\bar{q}$ pairs (i.e., by their valence partons), while the process independent distribution amplitude $\phi_\pi(x,Q)$ is just the probability amplitude for finding the $q\bar{q}$ Fock state in the pion (with $x_q = x$ and $x_{\bar{q}} = 1-x$): [15]

$$\phi_\pi(x,Q) = \int \frac{d^2k_\perp}{16\pi^3}\ \psi^{(Q)}_{q\bar{q}/\pi}(x,k_\perp). \qquad (3.2a)$$

$$= \int \frac{dz^-}{4\pi}\ e^{ixz^-/2} \langle 0|\bar{\psi}(0)\ \frac{\gamma^+\gamma_5}{2\sqrt{2}}\ \psi(z)|\pi\rangle^{(Q)}\Big|_{\substack{z^+ = z_\perp = 0 \\ P_\pi^+ = 1}} \qquad (3.2b)$$

The $k_\perp$ integration in (3.2) is cut off by the ultraviolet cut-off $\Lambda=Q$ implicit in $\psi_\pi^{(Q)}$; only Fock states with energies $|\varepsilon| \lesssim Q^2$ are important.

The distribution amplitude is only weakly dependent on Q, as is evident from the evolution equation

$$Q^2 \frac{\partial}{\partial Q^2}\ \phi_\pi(x,Q) = \int_0^1 dy\ V(x,y,\alpha_s(Q))\ \phi_\pi(y_i,Q). \qquad (3.3a)$$

$$V(x,y,\alpha_s(Q)) = \alpha_s(Q)\ V_1(x,y) + \alpha_s^2(Q) V_2(x,y) + \ldots$$

which we shall derive. The bulk of the Q dependence is in T_H. This hard scattering amplitude is defined to be collinear irreducible — i.e. all mass singularities are systematically subtracted out (and absorbed into the ϕ's). Therefore we can neglect all masses in T_H, leaving Q as the only scale. The amplitude must then have the general form

$$T_H(x_i, y_i, Q) = \frac{1}{Q^n} f(x_i, y_i, \alpha_s(Q)) \qquad (3.3b)$$

where, from simple dimensional arguments, n is the total number of initial and final partons less 4. The pion form factor (i.e. $e\pi \to e\pi$ where $n = 6 - 4$) falls as $1/Q^2$, up to logarithmic factors, according to this rule. A second consequence of neglecting masses is that total quark helicity is conserved in T_H when the gluons are vector bosons, as in QCD. Since ϕ carries no helicity, by its definition (3.2), the helicity of the hadron equals the sum of the helicities of its valence partons in T_H. Thus hadronic helicity is conserved in exclusive processes for large Q^2.

In the following sections we illustrate the derivation of these results by examining the pion form factor to leading order. We also examine some of the problems which arise in hadron-hadron scattering, certain baryon form factors, etc. due to various singularities in T_H. The phenomenological implications of this formalism are discussed by Stan Brodsky in his talks to this meeting.

B. An Example: The Meson Form Factor

The meson form factor (Eq.(2.17)) can be rewritten in terms of the

$q\bar{q}$ wave function alone (cf Eq.(2.15)):

$$F_\pi(Q^2) = \int \frac{dx\, d^2k_\perp}{16\pi^3} \int \frac{dy\, d^2\ell_\perp}{16\pi^3} \psi^{(\Lambda)*}(y,\ell_\perp) \frac{T(y,\ell_\perp;x,k_\perp;q_\perp)}{\sqrt{y(1-y)x(1-x)}} \psi^{(\Lambda)}(x,k_\perp) \qquad (3.4)$$

Here T is the sum of all $q\bar{q}$ irreducible LCPTh amplitudes for $\gamma^* + q\bar{q} \to q\bar{q}$ (Fig. 11), and the ultraviolet cut-off is $\Lambda^2 >> Q^2$.

Consider first the disconnected part of T (Fig. 11a), ignoring renormalization diagrams for the moment. It gives a contribution

$$\int_0^1 dx \int \frac{d^2k}{16\pi^3} \psi^{(\Lambda)*}(x,k_\perp + (1-x)q_\perp)\ \psi^{(\Lambda)}(x,k_\perp). \qquad (3.5)$$

to F_π. As $Q^2 = q_\perp^2 \to \infty$, two regions of phase space dominate in (3.5) —

a) $k_\perp << Q$ where $\psi^{(\Lambda)}(x,k_\perp)$ is large

b) $k_\perp + (1-x)q_\perp << Q$ where $\psi^{(\Lambda)*}(x,k_\perp + (1-x)q_\perp)$ is large

— since the wave functions are strongly peaked at low transverse momentum. In region a), $k_\perp$ can be neglected in $\psi^{(\Lambda)*}(x,k_\perp + (1-x)q_\perp)$ until $k_\perp \sim (1-x)Q$ at which point $\psi^{(\Lambda)*}$ begins to cut of the $k_\perp$ integration. Thus in region a), we can approximate (3.5) by

$$\int_0^1 dx\ \psi^{(\Lambda)*}(x,(1-x)q_\perp) \int^{(1-x)Q} \frac{d^2k_\perp}{16\pi^3} \psi^{(\Lambda)}(x,k_\perp) \qquad (3.6a)$$

— the bulk of the integral coming from $k_\perp^2 << Q^2 \to \infty$. Similarly we obtain

for region b)

$$\int_0^1 dx \{ \int_0^{(1-x)Q} \frac{d^2k_\perp}{16\pi^3} \psi^{(\Lambda)}(x,k_\perp)\}^* \psi^{(\Lambda)}(x,-(1-x)q_\perp) \qquad (3.6b)$$

These approximations are valid up to corrections of $O(1/\ell n\, Q^2)$ when $\psi \sim 1/k_\perp^2$, the crude expectation in QCD.

Eqs.(3.6) can be further simplified by using the bound state equation (2.6) for the valence wave function $\psi^{(\Lambda)}(x,(1-x)q_\perp)$:

$$\psi^{(\Lambda)}(x,(1-x)q_\perp) = \int_0^1 dy \int \frac{d^2\ell_\perp}{16\pi^3} \frac{V_{eff}(x,(1-x)q_\perp;y,\ell_\perp)}{-q_\perp^2 \frac{1-x}{x}} \psi^{(\Lambda)}(y,\ell_\perp)$$

As above, the dominant contribution here is from $\ell_\perp \ll Q(1-y)$, so we can approximate this equation by

$$\psi^{(\Lambda)}(x,(1-x)q_\perp) \simeq \int_0^1 dy \frac{V_{eff}(x,(1-x)q_\perp;y,0)}{-q_\perp^2 \frac{1-x}{x}} \int^{(1-y)Q} \frac{d^2\ell_\perp}{16\pi^3} \psi^{(\Lambda)}(y,\ell_\perp) \qquad (3.7)$$

to leading log order. It is readily demonstrated that the $q\bar{q}$ irreducible potential V_{eff} is free of mass singularities in light-cone gauge. Consequently all loop momenta are of order q or larger, and $V_{eff}(x,(1-x)q_\perp;y,0)$ can be computed perturbatively. Combining Eqs.(3.6) and (3.7) we arrive at a simple expression for (3.5):

$$\int_0^1 dx \int_0^1 dy\ \phi_0^*(y,(1-y)Q)\ \tilde{T}_H(y,x,Q)\ \phi_0(x,(1-x)Q) \qquad (3.8)$$

where the unrenormalized quark distribution amplitude ϕ_0 is

$$\phi_0(x,Q) \simeq \int^{Q^2} \frac{dk_\perp^2}{16\pi^2} \psi^{(\Lambda)}(x,k_\perp) \ , \qquad (3.9)$$

and $\tilde{T}_H$ is the LCPTh amplitude for $\gamma^* + q\bar{q} \to q\bar{q}$ depicted in Fig. 13 (divided by $\sqrt{y(1-y)x(1-x)}$).

In addition to (3.5), the connected parts T_c of T contribute to (3.4) as $Q \to \infty$. By the same reasoning used above, we can neglect $\ell_\perp$ and $k_\perp$ relative to $q_\perp$ in $T_c(y,\ell_\perp;x,k_\perp;q_\perp)$ to obtain a formula identical to (3.8) but with $\tilde{T}_H$ replaced by (Fig. 13)

$$\tilde{\tilde{T}}_H = \frac{T_c(y,0;x,0;q_\perp)}{\sqrt{y(1-y)x(1-x)}}$$

Again T_c is free of mass singularities (in $A^+ = 0$ gauge) and can be computed perturbatively. Still ignoring renormalization terms, the otherwise complete result is therefore

$$F_\pi^0(Q^2) \simeq \int_0^1 dx \int_0^1 dy \{ \phi_0^*(y,(1-y)Q)\ e_q T_H^0(y,x,Q)\ \phi_0(x,(1-x)Q) + \phi_0^*(y,yQ)\ e_{\bar{q}}\ T_H^0(1-y,1-x,Q)\ \phi_0(x,xQ)\} \tag{3.10}$$

where the hard scattering amplitude is to lowest order

$$T_H^0(y,x,Q) = \tilde{T}_H + \tilde{\tilde{T}}_H = \frac{16\pi C_F \alpha_s(\Lambda)}{Q^2}\ \frac{1}{(1-y)(1-x)}\ , \tag{3.11}$$

the Born amplitude for a collinear $q\bar{q}$ pair to scatter with the photon, and where the two terms in Eq.(3.10) arise from the photon hitting either the quark or the antiquark.

Finally we must consider the effects of vertex and propagator corrections in T_H(Fig.14). Each of these involves propagators off-shell by $\sim Q^2$ and so all loop momenta are of order Q or larger (in $A^+ = 0$ gauge). It is a trivial but important consequence of renormalizability that the bare

vertices and propagators are then modified only by factors[16]

$$\begin{aligned} &\frac{Z_i^{(\Lambda)}}{Z_i^{(Q)}} \qquad \text{for propagators} \\ &\frac{Z_i^{(Q)}}{Z_i^{(\Lambda)}} \qquad \text{for vertices} \end{aligned} \tag{3.12}$$

up to corrections of $O(\alpha_s(Q))$, where $Z_i^{(\Lambda)}$ and $Z_i^{(Q)}$ are the usual renormalization constants with ultraviolet cut-offs Λ and Q respectively. Thus in leading order T_H^o is replaced by (Fig.14)

$$\left[\frac{Z_{1F}^{(Q)}}{Z_{1F}^{(\Lambda)}}\right]^2 \frac{Z_3^{(\Lambda)}}{Z_3^{(Q)}}\, T_H^o = \left[\frac{Z_2^{(Q)}}{Z_2^{(\Lambda)}}\right]^2 \frac{\alpha_s(Q)}{\alpha_s(\Lambda)}\, T_H^o$$

where $Z_{1F}^{(\Lambda)}$ renormalizes quark-gluon vertices, and $Z_3^{(\Lambda)}$ and $Z_2^{(\Lambda)}$ renormalize the quark and gluon propagators. Here the photon-quark vertex correction cancels the quark propagator correction, by the Ward identity. We have also used the fact that $\alpha_s(\Lambda)\, Z_3^{(\Lambda)}(Z_2^{(\Lambda)}/Z_{1F}^{(\Lambda)})^2$ is Λ independent. So Eq.(3.10) is corrected to give

$$F_\pi(Q^2) = \int_0^1 dx \int_0^1 dy \, \{\phi^*(y,(1-y)Q)\, e_q T_H(y,x,Q)\, \phi(x,(1-x)Q) + (q \leftrightarrow \bar{q})\} \tag{3.13}$$

in leading order, where now

$$T_H(y,x,Q) = \frac{16\pi C_F \alpha_s(Q)}{Q^2} \frac{1}{(1-y)(1-x)} \tag{3.14}$$

and

$$\phi(x,Q) \simeq \frac{Z_2^{(Q)}}{Z_2^{(\Lambda)}} \int^{Q^2} \frac{dk_\perp^2}{16\pi^2} \psi^{(\Lambda)}(x,k_\perp). \tag{3.15}$$

Since the bulk of the integral in (3.15) comes from $k_\perp^2 \ll Q^2$, we can use Eq.(2.12) to redefine

$$\phi(x,Q) = \int \frac{d^2k_\perp}{16\pi^3} \psi^{(Q)}(x,k_\perp). \tag{3.16}$$

where now the $k_\perp$ cut-off (at $\sim Q$) is implicit rather than explicit. Eqs. (3.13)-(3.16) now have the general form proposed in the introduction (Eqs.(3.1)-(3.3)).

Comparing Eqs.(3.9) and (3.11) to Eqs.(3.16) and (3.14), we see that the major effect of the renormalization corrections is to replace $\alpha_s(\Lambda)$ by $\alpha_s(Q)$ and $\psi^{(\Lambda)}$ by $\psi^{(Q)}$. This is exactly what was expected from our general discussion of renormalization (Section 2.C). The only physical momentum scale in T_H is Q and so $\alpha_s(Q)$ is the natural expansion parameter. Furthermore T_H only probes structure in the wave functions down to distances of $O(1/Q)$. Thus the wave function $\psi^{(Q)}$, defined in the theory with cut-off Q, incorporates hadronic structure over all distance scales relevant to the physical process. Structure at distances much smaller than $1/Q$ is irrelevant except insofar as it determines $\alpha_s(Q)$, $m(Q)$ ... etc.

The leading order result (3.14) for T_H is consistent with the dimensional counting predictions for the pion form factor. These rules also show why it is that only the valence Fock state is relevant for large

Q^2. For example the hard scattering amplitude for scattering a $q\bar{q}q\bar{q}$ (collinear) state has four additional partons and so must fall as $1/Q^6$; this amplitude has many more far off-shell ($\sim Q^2$) internal propagators than does the $q\bar{q}$ amplitude. States with extra gluons must be treated with special care. For example the hard scattering amplitude in Fig. 15 has only one additional denominator ($\sim Q^2$), while the numerator is modified by a factor $\bar{u} \not{\epsilon} u \sim \epsilon \cdot q$ coupled to the gluon polarization ϵ. So this amplitude is suppressed by $\sim \epsilon \cdot q/Q^2$ which in light-cone gauge (i.e $\epsilon^+ = 0$) is $\epsilon \cdot q / Q^2 \sim \frac{1}{Q}$, in accordance with dimensional counting. However, other gauges can have $\epsilon \cdot q/Q^2 \sim \epsilon^+ q^-/Q^2 \sim \epsilon^+ Q^2/Q^2$ in which case the amplitude is not suppressed. In these gauges any number of A^+ gluons must be included in the pion Fock states, even in leading order. The absence of such spurious longitudinal gluons in light-cone gauge is another important advantage of this gauge.

C. The Quark Distribution Amplitude

All of the pion's low energy properties relevant for $F_\pi(Q^2)$ as $Q^2 \to \infty$ are lumped into the quark distribution amplitude $\phi(x,Q)$. Obviously ϕ is intrinsically non-perturbative. However its variation with Q can be studied perturbatively. To show this, we differentiate Eq.(3.15) with respect to Q^2:

$$Q^2 \frac{\partial}{\partial Q^2} \phi(x,Q) = \frac{Z_2^{(Q)}}{Z_2^{(\Lambda)}} \frac{Q^2}{16\pi^2} \psi^{(\Lambda)}(x,q_\perp) - \gamma_F(\alpha_s(Q))\, \phi(x,Q) \quad (3.17)$$

where γ_F is the anomalous dimension associated with $Z_2^{(Q)}$,

$$Q^2 \frac{d}{dQ^2} Z_2^{(Q)} = -\gamma_F(\alpha_s(Q))\, Z_2^{(Q)}$$
$$= -\{\frac{C_F \alpha_s(Q)}{2\pi} \int_0^1 dy\, \frac{1+(1-y)^2}{y} + O(\alpha_s^2(Q))\}\, Z_2^{(Q)} \qquad (3.18)$$

and $C_F = (n_c^2 - 1)/2n_c = 4/3$. The first term in (3.17) represents the change in the probability amplitude ϕ due to the addition of more $q\bar{q}$ states as Q increases, while the second reflects the loss of probability from those already present, as $Z_2^{(Q)}$ decreases. By using the bound state equation as in Eq.(3.7), we can express $\psi^{(\Lambda)}(x,q_\perp)$ in terms of $\phi(x,Q)$. To leading order we need only consider one-gluon exchange between the quark and anti-quark, which gives (Fig. 16)

$$\frac{Z_2^{(Q)}}{Z_2^{(\Lambda)}} \psi^{(\Lambda)}(x,q_\perp) = \frac{4\pi\alpha_s(Q)}{q_\perp^2} \int_0^1 \frac{dy}{y(1-y)} \tilde{V}(x,y)\, \phi(y,Q) \qquad (3.19)$$

where again $\alpha_s(\Lambda)$ is converted into $\alpha_s(Q)$ by propagator and vertex corrections. Substituting into Eq.(3.17), we finally obtain the evolution equation for ϕ

$$Q^2 \frac{\partial}{\partial Q^2} \phi(x,Q) = \frac{\alpha_s(Q)}{4\pi} \{\int_0^1 \frac{dy}{y(1-y)} V(x,y)\, \phi(y,Q) - \phi(x,Q)\} \qquad (3.20)$$

where

$$V(x,y) = 2C_F\{x(1-y)\theta(y-x)\left[\delta_{-h,\bar{h}} + \frac{\Delta}{y-x}\right] + \begin{bmatrix} x \leftrightarrow 1-x \\ y \leftrightarrow 1-y \end{bmatrix}\} = V(y,x)$$

with

$$\Delta \frac{\phi(y,Q)}{y(1-y)} \equiv \frac{\phi(y,Q)}{y(1-y)} - \frac{\phi(x,Q)}{x(1-x)}$$

and h, $\bar{h}$ the quark, antiquark helicities.

The evolution equation (3.20) completely determines the Q dependence of $\phi(x,Q)$; given $\phi(x,Q_o)$, $\phi(x,Q)$ is determined for any other Q by integrating this equation, numerically or otherwise. However it is instructive to exhibit explicitly the most general Q dependence. Using the symmetry $V(x,y) = V(y,x)$ to diagonalize V, the general solution of (3.20) is easily shown to be

$$\phi(x,Q) \simeq x(1-x) \sum_{n=0}^{\infty} a_n \, C_n^{3/2}(2x-1) \left\{ \ell n \frac{Q^2}{\Lambda_s^2} \right\}^{-\gamma_n/\beta_o} \tag{3.21}$$

where

$$\gamma_n = C_F\{1 + 4 \sum_{k=2}^{n+1} \frac{1}{k} - \frac{2\delta_{-h,\bar{h}}}{(n+1)(n+2)}\} \geq 0 \tag{3.22}$$

$$\beta_o = 11 - \frac{2}{3} n_f$$

and n_f is the number of quark flavors. (Λ_s here is the scale appearing in the running coupling constant — i.e. $\alpha_s(Q^2) = 4\pi/\beta_o \, \ell n(Q^2/\Lambda_s^2)$ — and has nothing to do with the ultraviolet cut-off Λ). By combining the orthogonality condition for the Gegenbauer polynomials $C_n^{3/2}$ with the definition (3.2) of ϕ, we arrive at an interpretation for the expansion constants in (3.21):

$$a_n\left[\ell n\frac{Q^2}{\Lambda^2}\right]^{-\gamma_n/\beta_o} = \frac{4(2n+3)}{(2+n)(1+n)}\int_0^1 dx\; C_n^{3/2}(2x-1)\;\phi(x,Q).$$

$$= \frac{4(2n+3)}{(2+n)(1+n)}\int_0^1 dx \int\frac{d^2k_\perp}{16\pi^3}\, C_n^{3/2}(2x-1)\;\psi^{(Q)}(x,k_\perp) \qquad (3.23)$$

$$= \frac{\sqrt{2}(2n+3)}{(2+n)(1+n)}\,\frac{1}{\sqrt{n_c}}\,\langle 0|\;\bar{\psi}(0)\gamma^+\gamma_5 C_n^{3/2}(i\overleftrightarrow{\partial}^+)\psi(0)\;|\pi\rangle^{(Q)}$$

where the matrix element of the local operator is evaluated with ultraviolet cut-off Q. Thus to leading order the pion's distribution amplitude has the simple form ($P_\pi^+ = 1$) [17]

$$\phi(x,Q) = x(1-x)\sum_{n=0}^{\infty}\frac{\sqrt{2}(2n+3)}{(2+n)(1+n)}\,\frac{1}{\sqrt{n_c}}\,C_n^{3/2}(2x-1)\,\langle 0|\;\bar{\psi}\gamma^+\gamma_5 C_n^{3/2}(i\overleftrightarrow{\partial}^+)\psi|\pi\rangle^{(Q)} \qquad (3.24)$$

Expansion (3.24) can also be derived directly from the operator product expansion of Eq.(3.2b) since the quark fields are on the light-cone ($z^2 = z^+z^- - z^2 = 0$).[18] This analysis has an important consequence which follows from (3.22). For very large Q^2 only the n=0 term remains in (3.24), so that

$$\phi(x,Q) \to \frac{3}{\sqrt{n_c}}\,x(1-x)\,\langle 0|\bar{\psi}\,\frac{\gamma^+\gamma_5}{\sqrt{2}}\psi|\pi\rangle^{(Q)} = \frac{3}{\sqrt{n_c}}\;f_\pi\;x(1-x) \qquad (3.25)$$

— i.e. $\phi(x,Q)$ is completely determined for very large Q. Actually this is just another way of writing Eq.(2.16), which gives a sum rule for $\phi(x,Q)$:

$$\int_0^1 dx\,\phi\,(x,Q) = \frac{f_\pi}{2\sqrt{n_c}} \qquad (3.26)$$

Given the shape of $\phi(x,Q)$, this equation normalizes if for any Q.

Notice finally from Eq.(3.19) that $\psi^{(\Lambda)}(x,q_\perp)$ does in fact fall as $1/q_\perp^2$, up to logarithms, as $q_\perp^2$ grows. The short distance behavior of the Fock state wave functions is perturbative in nature, and as a general rule is crudely that of simple Born diagrams in perturbation theory. In particular wave functions are not exponentially damped at large $q_\perp$ ($\gtrsim$ a GeV), as is frequently assumed in phenomenological analyses.

D. Complications

Exclusive processes at large Q^2 involve interactions of the hadronic constituents within a small volume near the light-cone, as is evident from Eqs.(3.24) and (3.2). This is due to the dynamical behavior of T_H, all of whose internal propagators are far off shell ($\sim Q^2$), and not simply due to kinematics as in deep inelastic scattering. Unfortunately the x integrations for certain processes can include points where internal lines in T_H go on-shell. In that case the long distance behavior of the theory obviously becomes relevant, and factorization as in Eq.(3.1) is jeopardized. These singularities in T_H can be of two types:

a) endpoint singularities which arise as $x \to 0$ or 1;

b) pinch singularities which occur in the middle of the integration region — i.e. $x \neq 0,1$.

We examine each in turn.

Endpoint singularities

The analysis of the $q\bar{q}$ contribution to $F_\pi(Q^2)$(Eq.(3.5)),

$$\int_0^1 dx \int \frac{d^2k}{16\pi^3} \psi^{(\Lambda)*}(x,k_\perp + (1-x)q_\perp)\psi^{(\Lambda)}(x,k_\perp) \ ,$$

depended upon the fact that either $k_\perp$ or $k_\perp + (1-x)q_\perp$ was of $O(q_\perp)$ — i.e. large momentum flowed through one or the other wave functions. This is obviously the case unless

$$1-x \lesssim \frac{\lambda}{q_\perp} \tag{3.27}$$

where $\lambda^2 \sim \langle k_\perp^2 \rangle$ is the mean $k_\perp^2$ in the wave functions. Within this infinitesimal region, called the endpoint region, both wave functions have small ($\sim\lambda^2$) transverse momenta. The form factor receives a contribution from this region of order

$$F(Q^2)_{EP} \sim \int_{1-\frac{\lambda}{Q}}^{1} dx \; |\psi^{(\Lambda)}(x,\lambda)|^2$$

$$\sim \left(\frac{\lambda}{Q}\right)\left(\frac{\lambda}{Q}\right)^{2\delta}$$

when $\psi^{(\Lambda)}(x,\lambda)$ vanishes as $(1-x)^\delta$ for $x \to 1$. This mechanism, in which spectator quarks are stopped rather than turned, was actually the first parton model suggested for hadronic form factors.[8] However, we expect the wave function's behavior to be perturbative when x is infinitesimally close to 1 (Fig.7), as discussed in Section 2.D (leading to Eq.(2.20)). Perturbation theory implies $\delta = 1$ and thus the endpoint contributions fall as $(\lambda/Q)^3$, down by a full power of λ/Q relative to the hard scattering contributions (Eq.(3.1)).

The analysis is similar for baryon form factors where

$$F(Q^2)_{EP} \sim \int_{1-\frac{\lambda}{Q}}^{1} dx_1 \int_0^{\lambda/Q} dx_2 \; |\psi^{(\Lambda)}(x_i,\lambda)|^2$$

$$\sim \left(\frac{\lambda}{Q}\right)^2\left(\frac{\lambda}{Q}\right)^{2\delta}$$

Perturbation theory again gives $\delta = 1$, but here the endpoint contribution seems to be suppressed by only two powers of $\alpha_s(\lambda Q)$ relative to the hard scattering prediction:

$$F_{EP} \sim \frac{\alpha_s^4(\lambda Q)}{Q^4} \sim \alpha_s^2(\lambda Q)\, F_{HS}$$

In fact the suppression is probably much stronger. The struck quark line is off shell by only $|\varepsilon| \sim \frac{\langle k_\perp^2 \rangle}{1-x} \sim \lambda Q \ll Q^2$ in the endpoint region. Thus radiative connections to the quark-photon vertex include double logarithms of Q^2 (i.e. $\alpha_s(\ell n Q^2)^2$) which exponentiate when summed to all orders, giving a quark form factor. This form factor falls as a power of λ/Q, further suppressing the endpoint contribution to the form factor.[19]

It must be emphasized that such 'Sudakov form factors' involve very low loop momenta ($\sim \lambda^2$) and may not be reliably analyzed in perturbation theory. On the other hand, the physics of a quark form factor which falls with increasing Q^2 transcends perturbation theory. A near on-shell (relative to Q^2) quark when struck by a highly virtual photon wants to radiate gluons, the amount of radiation increasing the more drastic is the change in the quark's state of motion. Thus the quark scattering amplitude is suppressed when such bremsstrahlung is prohibited, as it is in exclusive processes; i.e. we see the 'shadow' of the inelastic channels.

Note that double logs and Sudakov form factors do not appear in hard scattering amplitudes. This is because the collinear bunches of partons representing each hadron in T_H are color singlets, and the soft gluons which build up the Sudakov form factor decouple. In short, color singlets

need not radiate copiously when struck. In the endpoint region, however, the struck quark behaves as though isolated from the others (over time scales $\sim 1/\lambda Q$), and a Sudakov form factor does appear.

Finally notice that the presence of strong sensitivity to the endpoint region is usually evident from an inspection of the hard scattering amplitude, even in leading order. For example, $T_H(y,x,Q)$ for a pion (Eq.3.14) has linear singularities as either of x or y tends to 1. However the wave function's boundary conditions require that $\phi_\pi(x,Q)$ vanish like a power as $x \to 1$, so that Eq.(3.1) for $F_\pi(Q^2)$ never diverges. By contrast, the proton's magnetic form factor has a hard scattering form

$$G_M(Q^2) = \int dx_1\, dx_2 \int dy_1 dy_2\, \phi_p^*(y_i Q)\; T_H(y_i, x_i, Q)\phi_p(x_i, Q)$$

where T_H has a cubic singularity as $x_1 \to 1$. This expression could be singular even if ϕ_p vanishes as $x_1 \to 1$, resulting in the situation outlined above.

Pinch Singularities

The pinch singularity, first described by Landshoff, is most serious in hadron-hadron scattering. As an illustration consider the diagram in Fig. 17a, which contributes to π-π scattering. Three-momentum conservation requires ($s = r_\perp^2 + q_\perp^2$, $t = -q_\perp^2$, $u = -r_\perp^2$, $r_\perp \cdot q_\perp = 0$)

$$\begin{aligned} x_a + x_b &= x_c + x_d \\ k_a + k_b - k_c - k_d &= (x_c - x_a) r_\perp + (x_d - x_a)\, q_\perp \end{aligned} \tag{3.28}$$

where $k_a, \ldots, k_d$ are the transverse momenta appearing in the wave functions

$\psi^{(\Lambda)}(x,k)$. Clearly at least one of $k_a^2,..,k_d^2$ must be of order $s = r_\perp^2 + q_\perp^2$ for most values of $x_a,..,x_d$. Then, as in Section 3.B, the wave function with large $k_\perp$ is replaced by a gluon exchange to give a hard scattering amplitude, as depicted in Fig.17b (where k_a^2 is large). Dimensional counting implies

$$T_H \sim \frac{\alpha_s^3}{s^2} f(\theta_{CM}; x_a,...) \tag{3.29}$$

for this contribution. Also the energy denominator D in Fig.17a,

$$D = (x_c - x_a) r_\perp^2 + (x_d - x_a) q_\perp^2 + 2(k_d - k_a)\cdot q_\perp + 2(k_c - k_a)\cdot r_\perp + ... + i\varepsilon, \tag{3.30}$$

is of order s indicating that the two quark-quark scatterings occur within a very short time of each other ($\Delta\tau \sim 1/s$).

Notice however that in the 'pinch region'

$$|x_c - x_a| \lesssim \frac{\lambda}{r_\perp} \qquad |x_d - x_a| \lesssim \frac{\lambda}{q_\perp} \tag{3.31}$$

all wave function momenta $k_a^2,...$ can be small ($\sim \lambda^2$). Furthermore the denominator D is of order $\lambda\sqrt{s}$ or less, and can even vanish here. Thus the two quark-quark scatterings can occur more or less independently, at widely separated points. The scattering process is no longer localized, and factorization of the sort exhibited in Eq.(3.1) does not occur. The s dependence of the contribution from this region is readily estimated: a) the quark-quark scattering amplitudes give $(1/s)^0$, by dimensional counting; b) phase space as restricted by Eqs.(3.31) gives a factor $(\lambda/\sqrt{s})^2$; c) the energy denominator D gives a factor $1/D \sim 1/\lambda\sqrt{s}$. Thus the pinch region gives

$$T_{PS} \sim \frac{1}{s^{3/2}} f(\theta_{cm}; x_a)$$

which apparently dominates the hard scattering contributions (Eq.(3.29)) by a factor $\sqrt{s}$.

Two things work to suppress this pinch contribution. First the number of hard scattering amplitudes is much larger than the number of pinch singularity diagrams. More importantly, perhaps, radiative corrections to the individual quark-quark amplitudes build up Sudakov form factors which increase the effective power of $1/s$ to $\sim\frac{3}{2}+4\ C_F/\beta\ \ell n\ \ell n\sqrt{|t|/\lambda}(\to\infty$ as $|t|\sim s\to\infty)$; these corrections do not cancel here because the quarks and antiquarks scatter separately, and not together as color singlets. So the pinch region (3.31) is completely suppressed by Sudakov effects. Mueller has recently pointed out that a contribution still remains for hadron-hadron amplitudes from a region intermediate between the pinch region and the hard scattering region (e.g. for $k_a^2\sim\lambda^2(s/\lambda^2)^\delta \quad 0<\delta<1$). This results in a small correction to the power law predicted by dimensional counting; for example, pp elastic scattering at wide angles should fall off as $s^{-9.7}$, rather than s^{-10} as predicted by Eq.(3.3). The conservation of hadronic helicity is unaffected by these corrections.

When computing hard scattering contributions, pinch singularities appear as singularities in $T_H(x_a,x_b,..,Q)$at points $x_a,x_b,...$ away from the endpoints 0 and 1. The x integrals, with the distribution amplitudes, are then singular. If this singularity is only logarithmic, the integral is properly defined by a principal value prescription, thereby discarding the imaginary part of the amplitude (which is Sudakov suppressed). The pinch singularity causes no problem in this case. However, if the x integrals have power-law divergences, as in the $\pi\pi$ amplitude discussed

above, these must be cut-off by explicitly including Sudakov form factors in the pinch region (as always, Sudakov effects go away in the hard scattering region). Only the power law divergences lead to a modification of dimensional counting.

We end this section by tabulating the singularities that can occur for a variety of exclusive processes (M = meson; B = baryon):

Process	Endpoint Singularity	Pinch Singularity	
		Power	Logarithmic
$eM \to eM$			
$\gamma^* \gamma \to M$			
$\gamma\gamma \to M\bar{M}$			
$eB \to eB$	X		
$\gamma\gamma \to B\bar{B}$	X		
$\gamma B \to \gamma B$	X		X
$\gamma B \to MB$	X		X
$MB \to MB$	X	X	X
$BB \to BB$	X	X	X

Again we emphasize that the results of the previous sections are modified only for amplitudes with power-law pinch singularities, and even then only slightly modified.

4. HEAVY QUARK ATOMS

A. The Spectrum

Striking progress has been made in elucidating the structure and

properties of mesons containing heavy $Q\bar{Q}$ pairs, such as the $\psi,\psi',\ldots$ with $c\bar{c}$ pairs, and the $T,T',\ldots$ with $b\bar{b}$'s. The most prominent features of the spectra for such states are

a) only states having $Q\bar{Q}$ quantum numbers have been found — for example the levels of the $c\bar{c}$ system are in one to one correspondence with the low lying levels of positronium (curiously, many more states of charmonium have been produced experimentally than of positronium);

b) the heavy quarks move with non-relativistic velocities

$$\langle v_Q^2/c^2 \rangle \sim \frac{\Delta\varepsilon}{M_Q} \sim \begin{cases} .25 & \text{for } \psi \\ .1 & \text{for } T \end{cases}$$

where $\Delta\varepsilon \sim 500$ MeV is the mass difference between radial excitations;

c) non-relativistic potential models for $Q\bar{Q}$ pairs bound by an instantaneous interaction describe the spectra extremely well (better than 10%), and furthermore different parameterizations of the effective potential agree over distance scales relevant for the observed states (Fig. 18).[20]

This evidence strongly suggest that the $Q\bar{Q}$ Fock state is the dominant component of heavy quark mesons. It is this feature more than any other which has allowed us to make such progress in understanding these mesons. $Q\bar{Q}$ predominance is obviously mandatory for the success of potential models, relativistic or non-relativistic. Furthermore, as we shall see, it is of critical importance for the study of the various inclusive and exclusive decays of the heavy mesons.

Why are heavy quark mesons so different from π's,ρ's, ...? Why are

there not strong admixtures of purely light-quark Fock states like $q\bar{q}$, or of states with gluons like $Q\bar{Q}g$? The coupling between $Q\bar{Q}$ states and purely light-quark states can almost certainly be computed perturbatively since the Q and $\bar{Q}$ must annihilate, and this can only occur over a very short distance ($\sim 1/M_Q$). For example the $q\bar{q}$ wave function for a ψ or Υ is given to leading order by the amplitude in Fig. 19a; the probability for finding such a state is $\sim \alpha_s^6(M_Q) << 1$. Of course, this is just an example of the OZI suppression of quark flavor mixing. Similarly the amplitude for $Q\bar{Q}g$, with a hard gluon, is perturbative (Fig. 19b) and small. Perturbation theory fails us only for states in which the $Q\bar{Q}$ pair is accompanied by soft gluonic excitations (and the $q\bar{q}$ pairs they might produce).

The amplitude for such soft gluonic excitations has the usual form (Fig. 19c)

$$\psi_{Q\bar{Q}g} \sim \sum_{\substack{Q\bar{Q}g \\ (\text{soft})}} \frac{|Q\bar{Q}g\rangle\langle Q\bar{Q}g|\delta V|Q\bar{Q}\rangle}{E_{Q\bar{Q}} - E_{Q\bar{Q}g}} \tag{4.1}$$

where δV is the potential coupling quarks to the gluonic field (g represents a general gluonic excitation here). Gauge invariance requires that $\delta V \sim g_s \vec{P}_Q \cdot \vec{A}/M_Q$ for any gluonic field configuration (perturbative or otherwise), and thus matrix element $\langle Q\bar{Q}g|\delta V|Q\bar{Q}\rangle$ is of order $g_s\langle v_Q/c\rangle$, as is typical of E1 multipole transitions.[21] Squaring $\psi_{Q\bar{Q}g}$ and summing over all $Q\bar{Q}g$ states with soft 'gluons', we find that the phase space cancels the energy denominators, leaving a probability

$$\begin{aligned} P(Q\bar{Q}g) &= \sum_{\substack{Q\bar{Q}g \\ (\text{soft})}} |\psi_{Q\bar{Q}g}|^2 \\ &\sim \alpha_s \langle v_Q^2/c^2\rangle \end{aligned} \tag{4.2}$$

for finding a $Q\bar{Q}$ together with any soft excitation in the color fields. So such non-perturbative higher Fock states are suppressed by $\langle v_Q^2/c^2\rangle$ in non-relativistic $Q\bar{Q}$ bound states — slowly moving quarks don't radiate much.

(An analogous situation arises in the hydrogen atom, which has a small admixture of $ep\gamma$ Fock states with $P(ep\gamma) \sim \alpha(v_e/c)^2 \sim \alpha^3$ for soft photons. These Fock states, with photon energies of order the binding energy ($k_\gamma \sim \alpha^2 m_e$), are directly responsible for the Lamb shift, which is then readily estimated: $\Delta E_{LS} \sim P(ep\gamma)\langle ep\gamma|H|ep\gamma\rangle \sim \alpha^3(\alpha^2 m)$. Clearly the hydrogen atom is well represented by just the ep Fock state to a very high degree of accuracy.)

Armed with this intuitive understanding of $Q\bar{Q}$ systems, we now examine a variety of detailed aspects of these mesons and their interactions, with the dual purposes of a) developing further intuition about the non-perturbative interactions at work in $Q\bar{Q}$ mesons, and b) using $Q\bar{Q}$ systems as a testing ground for perturbative QCD.

B. The Potential

Given that higher Fock states are not very important, we expect a $Q\bar{Q}$ interaction potential which is instantaneous — retardation effects should be unimportant (cf Eq.(2.7)). We have some guidance in constructing this potential from strong coupling ($r \to \infty$) and weak coupling ($r \to 0$) expansions in QCD,

$$V(r) \to \begin{cases} Kr & r \to \infty \\ \dfrac{\alpha_s(1/r)}{r} & r \to 0 \end{cases} \qquad (4.3)$$

though it is clear that neither form adequately describes current data.

However surprisingly simple interpolations for V(r) work very well. One of the best is due to Richardson who takes (in momentum space):

$$V(\vec{q}) = \frac{(4\pi)^2}{\beta_0} \frac{1}{\vec{q}^2 \ell n(1+\vec{q}^2/\Lambda_s^2)}$$

$$\rightarrow \begin{cases} \dfrac{(4\pi)^2 \Lambda^2}{\beta_0 \vec{q}^4} & \vec{q}^2 \rightarrow 0 \\ \dfrac{4\pi\alpha_s(q)}{\vec{q}^2} & \vec{q}^2 \rightarrow \infty \end{cases} \qquad (4.4)$$

A refined version of this potential gives a good fit to all ψ and Υ energy levels with a QCD scale parameter (in $\overline{MS}$ scheme) $\Lambda_s \rightarrow \Lambda_{\overline{MS}} \sim$ 200-500 MeV which is in reasonable agreement with other determinations of $\Lambda_{\overline{MS}}$.[20] However there is very little theoretical justification for such potentials, so a measure of skepticism is well warranted. One thing is clear though: the $Q\bar{Q}$ interaction is still definitely non-perturbative even at $Q^2 \sim \langle P^2 \rangle_T \sim$ 2 GeV^2. Thus any detailed perturbative calculations is probably unreliable at these Q^2's.

There has also been recent work on the spin dependent interactions in heavy quark mesons. Buchmüller et al have investigated the hyperfine splitting of s-states in perturbation theory (Fig. 20a). They find a potential (in momentum space)[22]

$$V_{HFS}(q) = \frac{32}{9\pi} \frac{\alpha_{\overline{MS}}(q)}{M_Q^2} \vec{s}_1 \cdot \vec{s}_2 \{1$$

$$+ \frac{\alpha_{\overline{MS}}(q)}{\pi} [-3.186 + \frac{5}{12}\beta_0 + \frac{21}{8} \ell n(q^2/M_Q^2)]\} \qquad (4.5)$$

for s-states ($\beta_0 = 11 - \frac{2}{3}n_f$ with n_f = number of massless quark flavors and $\alpha_{\overline{MS}}$ designates the $\overline{MS}$ definitions of α_s). This result is interesting in several ways. The first is that it works. Using measured ratios of the ψ-η_c mass difference to the widths $\Gamma(\psi \to e\bar{e}, \mu\bar{\mu})$ and $\Gamma(\eta_c \to \text{hadrons})$, these authors obtain a QCD scale parameter $\Lambda_{\overline{MS}} = 160 \pm 20$ MeV (with unknown theoretical errors). This is again in good agreement with other determinations. The next point of interest is that the hyperfine interaction is not really a short distance effect. From Eq.(4.5), the leading order shift is proportional to

$$\int d^3q\, d^3k\, \psi^*(k)\, \alpha_{\overline{MS}}(|\vec{k}-\vec{q}|)\, \psi(q)$$

and so the typical momentum in $\alpha_{\overline{MS}}$ is of order the mean $Q\bar{Q}$ momentum (and not $M_{Q\bar{Q}}$). Given that the spin independent interactions are non-perturbative for ψ's and Υ's, there seems a little <u>a priori</u> reason to use perturbation theory for the hyperfine interaction in these mesons.

Finally the $\ell n(q^2/M_Q^2)$ in Eq.(4.5) indicates sensitivity to low momenta. Such logarithms are generally accompanied by an additive constant of O(1) due to an infinity of diagrams — in this case diagrams in which the $Q\,\bar{Q}$ interact arbitrarily often while a soft gluon ($k_g \sim \Delta\varepsilon$, the level spacing) propagates near mass-shell (Fig.20b), in close analogy to the QED Lamb Shift.[23] The calculation is not complete until these have been computed. That such behavior should appear in the $Q\bar{Q}$ hyperfine interactions is not surprising given that the interaction of a quark with a uniform external chromomagnetic field is similarly non-perturbative.[23] Like the Lamb shift, these terms are due to the coupling with higher Fock states — here to $Q\bar{Q}g$ states where the gluon is soft. It will be very interesting to see

how well Eq.(4.5) describes the T-η_b splittings, since relativistic corrections and non-perturbative effects here are much less important than at the ψ. In the meantime, a better theoretical understanding even within perturbation theory is needed.

C. Inclusive Decays — s-states

The total decay rate of the T into hadrons is particularly simple to analyze because the annihilation of the heavy quarks occurs over distances much smaller than either the average $b\bar{b}$ separation in the T, or the typical distances over which the final state quarks and gluons are converted into hadrons (i.e. the color confinement radius). As a result, the leading order amplitude factors,[24]

$$\begin{aligned}\Gamma_0(T \to \text{hadrons}) &\simeq |\psi_{NR}(0)|^2\ \Gamma(b\bar{b} \to ggg)\ P(ggg \to \text{hadrons}) \\ &\simeq |\psi_{NR}(0)|^2\ \frac{160(\pi^2 - 9)}{81\ M_T^2}\ \alpha_s^3(M_b)\ ,\end{aligned} \tag{4.6}$$

where the factors have the following interpretations:

$|\psi_{NR}(0)|^2$ — the non-relativistic wave function at the origin, which is the probability that the quark and anti-quark are sufficiently close to annihilate (i.e. $r \sim 1/M_b \sim 0$ relative to $\langle r \rangle_T$);

$\Gamma(b\bar{b} \to ggg)$ — the decay rate for a stationary (since $\langle P_{Q_T}^2 \rangle \ll M_Q^2$) $Q\bar{Q}$ pair into gluons, which can be computed perturbatively (Fig.21a) since the decay occurs at short distances;

$P(ggg \to \text{hadrons})$ — the probability that the gluons convert into color singlet hadrons (=1), which can only factor in this way when there are no strong resonances between the initial gluons (i.e. when the final state configurations are predominantly jet-like with three gluon-jets).

Here the long distance structure of the meson figures only in the overall factor $|\psi_{NR}(0)|^2$.

The corrections to this simple result come from several sources. There are $O(v_b^2/c^2)$ corrections due to relativistic kinematics, as well as from spin-orbit, spin-spin and similar interactions. These might contribute at the 10-20% level for the Υ. Potentially more serious are contributions due to higher Fock states — e.g. decay through the channels $b\bar{b}g \to ggg$ where the gluon in the initial Fock state is very soft ($\sim \Delta\varepsilon$) and non-perturbative (Fig.21b). Such a contribution is of order the probability of finding a $b\bar{b}g$ in the Υ (Eq.(4.2)) times the decay rate $\Gamma(b\bar{b}g \to ggg)$. The final annihilation of the heavy quarks is suppressed by $\langle v_b^2/c^2 \rangle$ here, because the quarks are in a p-state after having emitted a soft gluon to form the $b\bar{b}g$ state (via an E1 transition), and p-state wave functions vanish at the origin (Section 4.D). Thus the contribution to Υ decay from these Fock states is most likely negligible, being only of order [25]

$$P(b\bar{b}g)\ \Gamma(b\bar{b}g \to ggg) \sim \frac{\alpha_s(\Delta\varepsilon)}{\alpha_s(M)} \left\langle \left(\frac{v}{c}\right)^4 \right\rangle \Gamma_0 << \Gamma_0 \qquad (4.7)$$

where Γ_0 is the leading order result (4.6).

One final source of corrections to (4.6) are the radiative corrections to the rate $\Gamma(b\bar{b}\to ggg)$ (these allow $b\bar{b}\to gggg, ggq\bar{q}$ as well). The leading radiative corrections involve relativistic loop momenta ($\sim M_b$) and so the dominant interactions are perturbative. These contributions have recently been computed[26]

$$\Gamma(\Upsilon\to \text{hadrons}) = |\psi_{NR}(0)|^2 \frac{160(\pi^2-9)}{81\, M_\Upsilon^2}\alpha_{\overline{MS}}(M)\left[1+\frac{\alpha_{\overline{MS}}(M)}{\pi}\{-19.3(5) + \frac{3}{2}\beta_0[1.154(5)+\ell n(2M/M_\Upsilon)]\}+\ldots\right] \tag{4.8}$$

where again $\beta_0 = 11-\frac{2}{3}n_f$ and n_f is the number of light-quark flavors (=4 for Υ). In this equation, we assume that the wave function ψ_{NR} contains the effects of all relevant long-distance non-perturbative $Q\bar{Q}$ interactions, and of the non-relativistic Coulomb interaction (corrected for the running coupling constant). This needn't concern us however if we compare the decay rate into hadrons with the rate into $\mu^+\mu^-$ pairs, which from a similar analysis is given by

$$\Gamma(\Upsilon\to\mu^+\mu^-) = 16\pi e_b^2\,\alpha_{QED}^2\,\frac{|\psi_{NR}(0)|^2}{M_\Upsilon^2}\left[1-\frac{16}{3}\frac{\alpha_{\overline{MS}}(M)}{\pi}\right]$$

where e_b is the quark charge (in units of e). By forming a ratio, all dependence on ψ_{NR} cancels, leaving an unambiguous prediction of perturbative QCD:

$$\frac{\Gamma(\Upsilon\to\text{hadrons})}{\Gamma(\Upsilon\to\mu^+\mu^-)} = \frac{10(\pi^2-9)}{81\,\pi\, e_b^2}\,\frac{\alpha_{\overline{MS}}^3(M)}{\alpha_{QED}^2}\left[1+\frac{\alpha_{\overline{MS}}(M)}{\pi}\{-14.0(5) + \frac{3}{2}\beta_0[1.154(5)+\ell n(2M/M_\Upsilon)]\}\ldots\right] \tag{4.9}$$

Equations (4.8) and (4.9) are independent of the choice of $M(\sim M_b)$. up to corrections of $O(\alpha_{\overline{MS}}^2/\pi^2)$. A particularly convenient choice for comparison with data is $M = 0.48(2)M_T$ as then the $O(\alpha_{\overline{MS}})$ corrections in Eq. (4.9) vanish (although this may be somewhat misleading, as discussed in Appendix B). Excellent data exists for this ratio providing one of the best determinations of the QCD coupling constant and scale parameter:

$$\alpha_{\overline{MS}}(0.48\ M_T) \simeq 0.158^{+\ 0.012}_{-\ 0.010}$$
$$\Lambda_{\overline{MS}} \simeq 100^{+\ 34}_{-\ 25}\ \text{MeV} \qquad (4.10)$$

where the errors are experimental. Similar results are obtained for ψ and ψ' decays, although v^2/c^2 corrections could be quite substantial for these ($\sim$ factor of 2?). Indeed the consistency of the ψ and Υ analyses implies empirical limits on the uncertainties due to v^2/c^2 corrections, higher Fock states, and higher orders in α_s; these limits are crudely ±20%, for the decay rate, i.e. on the order of the experimental uncertainties.

A number of other s-state decays have been analyzed, of which perhaps the most interesting for QCD is the ratio[27]

$$\frac{\Gamma(\eta_c \to \text{hadrons})}{\Gamma(\eta_c \to \gamma\gamma)} = \frac{2}{9e_c^4}\ \frac{\alpha_{\overline{MS}}^2(M\eta_c)}{\alpha_{QED}^2}\ \left[1 + \frac{\alpha_{\overline{MS}}(M\eta_c)}{\pi}\ \{2.46 + \frac{4}{3}\ \beta_o\}\right] \qquad (4.11)$$

Several of these rates are tabulated in Table I. Wave functions from Ref.20 are used to predict absolute rates.

TABLE I

Process	Theory (keV)	Experiment (keV)
$\Gamma(T \to \text{hadrons})$	28±6	27±7
$\Gamma(T \to \mu^+\mu^-)$	1.2±0.2	1.16±0.15
$\Gamma(T \to \gamma + \text{hadrons})$	0.9±0.2	...
$\Gamma(\eta_b \to \text{hadrons})$	6±1	...
$\Gamma(T \to \text{hadrons})$	80±40	44±6
$\Gamma(\psi \to \mu^+\mu^-)$	5±3	4.8±0.6
$\Gamma(\psi \to \gamma + \text{hadrons})$	7.5±4	...
$\Gamma(\eta_c \to \text{hadrons})$	17±8 MeV	$\lesssim$ 20 MeV

Estimates for the decays of heavy quark mesons. The theoretical errors represent crude estimates of the uncertainties due to v^2/c^2,... corrections.

D. Inclusive Decays — P-states

As mentioned earlier, hadronic decay rates for heavy quarks in a p-state are suppressed relative to s-state rates by $\langle v^2/c^2 \rangle$; the decay rates are proportional to $|\frac{d}{dr} \psi_{NR}(0)|^2$ rather than $|\psi_{NR}(0)|^2$ which vanishes for p-states. Because of this, decay via higher Fock states like $Q\bar{Q}g$ is not suppressed at all.[28] For example, the $P(1^{+-})$ state decays into three gluons in lowest order with a rate of order $\langle v_Q^2/c^2 \rangle \Gamma(s \to ggg)$ where $\Gamma(s \to ggg)$ is the rate for an s-state. As for s-states (Section 4.C), we estimate the rate due to Fock state $Q\bar{Q}g$ by $P(Q\bar{Q}g)\ \Gamma(Q\bar{Q}g \to ggg)$, but here the quarks in the $Q\bar{Q}g$ state are in an s-state (Fig. 21c) and the annihilation is not suppressed. Thus $P(Q\bar{Q}g)\ \Gamma(Q\bar{Q}g \to ggg)$ is of order $\langle v_Q^2/c^2 \rangle \Gamma(s \to ggg)$ as well, in marked contrast with Eq.(4.7); and soft non-perturbative gluonic excitations (Fig. 21c) contribute even in leading order for this p-state.

This sensitivity to soft gluons is readily apparent in perturbation theory. The leading order decay rate for the $P(1^{+-})$ state, for example, is proportional to $\alpha_s^3\ \ell n(M_Q/\varepsilon)$ where ε is the binding energy.[29] Just as for the hyperfine interaction (Section 4.B), the presence of a logarithm indicates infrared sensitivity. Furthermore even in perturbation theory there will be an infinity of diagrams which contribute to the same order (Fig. 21d), as was the case for the hyperfine structure. These logarithms, and the difficulties associated with them plague all p-state decays, rendering the theory of these decays much less reliable than that for s-states. On the other hand an understanding of the gluonic excitations in heavy quark systems is desirable and the properties of

these decays could provide useful insight.

E. QED Radiative Decays

Perhaps the most serious outstanding problem for the standard analysis of heavy-quark mesons is the failure (by factors of 2-3) of the predictions for E1 transitions like $\psi' \to \gamma\chi$. The leading order effect comes from the diagram in Fig. 22a. The loop integration is completely non-relativistic so the wave functions enter in precisely the region where they are best known.

There are basically two sorts of corrections which might arise. First there are kinematical corrections of $O(v_Q^2/c^2)$ due to relativity. These might well be very significant for $c\bar{c}$ states, but probably not for $b\bar{b}$ mesons. Secondly there are gluonic corrections to the basic diagram (Fig. 22b); but these are really just corrections due to higher Fock states — $Q\bar{Q}g$, $Q\bar{Q}gg$,... — as illustrated in Fig. 22b. Remembering that it is the non-relativistic region that is probed by these decays, these Fock states can hardly be important here and unimportant in determining the spectrum. In other words corrections of this second type can only be important if there are significant retardation effects in the basic $Q\bar{Q}$ potential. E1 transition rates for the T system which disagree with theory by factors of 2-3 would seriously challenge the validity of the simple $Q\bar{Q}$ model currently accepted.

F. QCD Radiative Decays

The coupling of soft gluonic excitations to the $Q\bar{Q}$ system was an important element in much of the previous discussion. Our intuition

concerning this coupling can be directly tested by examining QCD radiative transitions like (Fig. 23)

$$\Upsilon' \to \Upsilon + \text{gluons}$$
$$\qquad\qquad\qquad \lfloor_{\to}\ \pi\pi, \eta$$

Some time ago Gottfried pointed out that the gluons in such a process have wavelengths much longer than the mean radius of the meson. Thus the gluon-meson coupling might be dominated by the leading terms in a multipole expansion of the gluonic field.[30] For example, $\psi' \to \psi\pi\pi$ would involve a double E1 transition, while $\psi' \to \psi\eta$ would proceed via an M1M1 or E1M2 transition. This idea implies scaling relations between different processes — e.g.

$$\frac{\Gamma(\Upsilon' \to \Upsilon\pi\pi)}{\Gamma(\psi' \to \psi\pi\pi)} \sim \left(\frac{\langle r^2\rangle_{\Upsilon'}}{\langle r^2\rangle_{\psi'}}\right)^2 \sim \frac{1}{16}$$

since an E1 coupling is proportional to r; also $\Gamma(\Upsilon' \to \Upsilon\eta) << \Gamma(\Upsilon' \to \psi\pi\pi)$ because an M1M1 or E1M2 transitions is higher order in the multipole expansion than an E1E1 transitions. These relations work surprisingly well.

Recently Kuang and Yan made a detailed model which incorporates effects due to the multipole couplings, phase space, PCAC, the $Q\bar{Q}g$ intermediate states, and a variety of $Q\bar{Q}$ potentials.[31] Using data for $\psi' \to \psi\pi\pi, \psi\eta$ as inputs they predicted rates, $\pi\pi$ mass distributions, and angular correlations for a number of Υ transitions. Some of these predictions are shown in Table II, together with recent experimental results. The agreement is impressive given our primitive understanding of these

TABLE II

Theoretical and experimental results for QCD radiative transitions in the T system.

Transition	Γ(keV)	Branching Ratio (Theory)	Branching Ratio (Experimental)[32]
$T' \to T\pi^+\pi^-$	4-5	17-20%	19±3%
$T' \to T\eta$	.01	.04	5±2
$T'' \to T\pi^+\pi^-$	.2-.6	1-4	<17.5
$T'' \to T'\pi^+\pi^-$	.3-.5	1-2	
$T'' \to T\eta$	.003-.005	.02-.03	
$T'' \to (1^1P_1)\pi\pi$	.1-.2		
$(2\ ^3P_\gamma) \to (1'^3S_0)\pi\pi$	.6-3		

non-perturbative interactions; and it lends further credence to our previous discussions of $Q\bar{Q}g$ Fock states in heavy-quark mesons.

G. Summary

As we have seen there is abundant evidence suggesting that the ψ and T systems are predominantly $Q\bar{Q}$ bound states with little admixtures of higher Fock states. The quantum numbers, the success of the non-relativistic potential models, and the successes of the multipole expansion for hadronic transitions all argue in favor of this picture. Given this, we can use $Q\bar{Q}$ states as a laboratory for studying and testing QCD. The spectrum of states in effect measures the $Q\bar{Q}$ potential as a function of r. The s-state decays determine the QCD coupling constant and provide information about the gluon and gluon jets. In some ways these systems are the best for testing QCD because we know so much about their internal structure. The uncertainties due to bound state effects in T decay are probably much better under control than those due to higher twist corrections in deep inelastic scattering. Finally these systems may provide useful sources for exotic physics — e.g. $t\bar{t} \rightarrow \text{Higgs} + \gamma$.

Note added in Proof: A detailed analysis suggests that higher order diagrams such as in Fig. 20b. do not, in fact, contribute to the $O(\alpha_s)$ corrections in the hyperfine splitting for $Q\bar{Q}$ mesons. While individual diagrams seem important in Feynman gauge, these cancel when all diagrams are considered; such spurious terms never appear in Coulomb gauge. The discussion of the hadronic decays of p-states (section 4d) remains unchanged.

Appendix A — Light Cone Quantization and Perturbation Theory

In this Appendix, we outline the canonical quantization of QCD in $A^+ = 0$ gauge. This proceeds in several steps. First we identify the independent dynamical degrees of freedom in the Lagrangian. The theory is quantized by defining commutation relations for these dynamical fields at a given light-cone time $\tau = t + z$ (we choose $\tau = 0$). These commutation relations lead immediately to the definition of the Fock state basis. Expressing dependent fields in terms of the independent fields, we then derive a light-cone Hamiltonian, which determines the evolution of the state space with changing τ. Finally we derive the rules for τ-ordered perturbation theory.

The major purpose of this exercise is to illustrate the origins and ture of the Fock state expansion, and of light-cone perturbation theory. We will ignore subtleties due to the large scale structure of non-abelian gauge fields (e.g. 'instantons'), chiral symmetry breaking, and the like. Although these have a profound effect on the structure of the vacuum, the theory can still be described with a Fock state basis and some sort of effective Hamiltonian. Furthermore the short distance interactions of the theory are unaffected by this structure, or so at least is the central ansatz of perturbative QCD.

Quantization

The Lagrangian (density) for QCD can be written

$$\mathcal{L} = -\tfrac{1}{2}\mathrm{Tr}(F^{\mu\nu}F_{\mu\nu}) + \bar{\psi}(i\not{\partial} - m)\psi \qquad (A.1)$$

where $F^{\mu\nu} = \partial^\mu A^\nu - \partial^\nu A^\mu + ig[A^\mu, A^\nu]$ and $iD^\mu = i\partial^\mu - gA^\mu$. Here the gauge field A^μ is a traceless 3x3 color matrix ($A^\mu \equiv \sum_a A^{a\mu} T^a$, $\mathrm{Tr}(T^a T^b) = \frac{1}{2}\delta^{ab}$, $[T^a, T^b] = ic^{abc}T^c, \ldots$), and the quark field ψ is a color triplet spinor (for simplicity, we include only one flavor). At a given light-cone time, say $\tau=0$, the independent dynamical fields are $\psi_+ \equiv \Lambda_+\psi$ and $A^i_\perp$ with conjugate fields $i\psi^\dagger_+$ and $\partial^+ A^i_\perp$, where $\Lambda_\pm = \gamma^0\gamma^\pm/2$ are projection operators ($\Lambda_+\Lambda_- = 0$, $\Lambda_\pm^2 = \Lambda_\pm$, $\Lambda_+ + \Lambda_- = 1$) and $\partial^\pm = \partial^0 \pm \partial^3$. Using the equations of motion, the remaining fields in $\mathcal{L}$ can be expressed in terms of ψ_+, $A^i_\perp$:

$$\begin{aligned}
\psi_- \equiv \Lambda_-\psi &= \frac{1}{i\partial^+}\,[i\vec{D}_\perp\cdot\vec{\alpha}_\perp + \beta m]\psi_+ \\
&= \tilde{\psi}_- - \frac{1}{i\partial^+}\, g\,\vec{A}_\perp\cdot\vec{\alpha}_\perp\,\psi_+ \\
A^+ &= 0 \qquad\qquad (A.2)\\
A^- &= \frac{2}{i\partial^+}\, i\vec{\partial}_\perp\cdot\vec{A}_\perp + \frac{2g}{(i\partial^+)^2}\{[i\partial^+ A^i_\perp, A^i_\perp] + 2\,\psi^\dagger_+ T^a \psi_+ T^a\} \\
&\equiv \tilde{A}^- + \frac{2g}{(i\partial^+)^2}\{[i\partial^+ A^i_\perp, A^i_\perp] + 2\,\psi^\dagger_+ T^a\,\psi_+\,T^a\}
\end{aligned}$$

with $\beta = \gamma^0$ and $\vec{\alpha}_\perp = \gamma^0\vec{\gamma}_\perp$.

To quantize, we expand the fields at $\tau=0$ in terms of creation and annihilation operators,

$$\begin{aligned}
\psi_+(x) &= \int_{k^+>0} \frac{dk^+ d^2k_\perp}{k^+ 16\pi^3} \sum_\lambda \{\, b(\underline{k},\lambda)u_+(\underline{k},\lambda)\, e^{-ik\cdot x} \\
&\qquad + d^\dagger(\underline{k},\lambda)v_+(\underline{k},\lambda)e^{ik\cdot x}\}_{\tau = x^+ = 0} \qquad (A.3)\\
A^i_\perp(x) &= \int_{k^+>0} \frac{dk^+ d^2k_\perp}{k^+ 16\pi^3} \sum_\lambda \{a(\underline{k},\lambda)\varepsilon^i_\perp(\lambda)\, e^{-ik\cdot x} + \text{c.c.}\}_{\tau = x^+ = 0}\,,
\end{aligned}$$

with commutation relations ($\underline{k} = (k^+, \vec{k}_\perp)$):

$$\begin{aligned} \{b(\underline{k},\lambda),\, b^\dagger(\underline{p},\lambda')\} &= \{d(\underline{k},\lambda),\, d^\dagger(\underline{p},\lambda')\} \\ &= [a(\underline{k},\lambda),\, a^\dagger(\underline{p},\lambda')] \\ &= 16\pi^3 k^+ \delta^3(\underline{k} - \underline{p})\delta\lambda\lambda' \\ \{b,b\} = \{d,d\} &= \ldots = 0 \end{aligned} \tag{A.4}$$

where λ is the quark or gluon helicity. These definitions imply canonical commutation relations for the fields with their conjugates ($\tau = x^+ = y^+ = 0$, $\underline{x} = (x^-, x_\perp)$, ...):

$$\begin{aligned} \{\psi_+(\underline{x}), \psi_+^\dagger(\underline{y})\} &= \Lambda_+ \delta^3(\underline{x}-\underline{y}) \\ [A^i(\underline{x}), \partial^+ A_\perp^j(\underline{y})] &= i\delta^{ij}\delta^3(\underline{x}-\underline{y}) \end{aligned} \tag{A.5}$$

As described in Section 2.A, the creation and annihilation operators define the Fock state basis for the theory at $\tau=0$, with a vacuum $|0\rangle$ defined such that $b|0\rangle = d|0\rangle = a|0\rangle = 0$. The evolution of these states with τ is governed by the light-cone Hamiltonian, $H_{LC} = P^-$, conjugate to τ. Combining Eqs.(A.1) and (A.2), the Hamiltonian is readily expressed in terms of ψ_+ and $A_\perp^i$:

$$H_{LC} = H_0 + V$$

where

$$H_0 = \int d^3\underline{x}\, \{\mathrm{Tr}\,(\partial_\perp^i A_\perp^j \partial_\perp^i A_\perp^j) + \psi_+^\dagger (i\partial_\perp \cdot \alpha_\perp + \beta m) \frac{1}{i\partial^+} (i\partial_\perp \cdot \alpha_\perp + \beta m)\, \psi_+\}$$

$$= \sum_{\substack{\lambda \\ \text{colors}}} \int \frac{dk^+ d^2k_\perp}{16\pi^3 k^+} \{a^\dagger(\underline{k},\lambda) a(\underline{k},\lambda) \frac{k_\perp^2}{k^+} + b^\dagger(\underline{k},\lambda) b(\underline{k},\lambda) \frac{k_\perp^2+m^2}{k^+} + d^\dagger(\underline{k},\lambda) d(\underline{k},\lambda) \frac{k_\perp^2+m^2}{k^+}\} + \text{constant} \tag{A.6a}$$

is the free Hamiltonian and V the interaction:

$$V = \int d^3\underline{x}\{2g\ \mathrm{Tr}(i\partial^\mu\tilde{A}^\nu[\tilde{A}_\mu,\tilde{A}_\nu]) - \frac{g^2}{2}\mathrm{Tr}([\tilde{A}^\mu,\tilde{A}^\nu][\tilde{A}_\mu,\tilde{A}_\nu])$$
$$+ g\,\bar{\tilde{\psi}}\tilde{\not{A}}\tilde{\psi} + g^2\mathrm{Tr}([i\partial^+\tilde{A}^\mu,\tilde{A}_\mu]\frac{1}{(i\partial^+)^2}[i\partial^+\tilde{A}^\nu,\tilde{A}_\nu]) \qquad \text{(A.6b)}$$
$$+ g^2\bar{\tilde{\psi}}\tilde{\not{A}}\frac{\gamma^+}{2i\partial^+}\tilde{\not{A}}\tilde{\psi} - g^2\bar{\tilde{\psi}}\gamma^+(\frac{1}{(i\partial^+)^2}[i\partial^+\tilde{A}^\mu,\tilde{A}_\mu])\tilde{\psi}$$
$$+ \frac{g^2}{2}\bar{\psi}\gamma^+T^a\psi\frac{1}{(i\partial^+)^2}\bar{\psi}\gamma^+T^a\psi\}$$

with $\tilde{\psi} = \tilde{\psi}_- + \psi_+$ ($\to\psi$ as $g\to 0$) and $\tilde{A}^\mu = (0,\tilde{A}^-,\tilde{A}^i_\perp)$ ($\to A^\mu$ as $g\to 0$). The Fock states are obviously eigenstates of H_o with

$$H_o|n:\ k_i^+,k_{\perp i}> = \sum_i\left(\frac{k_\perp^2+m^2}{k^+}\right)_i |n:k_i^+,k_{\perp i}> \qquad \text{(A.7)}$$

It is equally obvious that they are not eigenstates of V, though any matrix element of V between Fock states is trivially evaluated. The first three terms in V correspond to the familiar three and four gluon vertices, and the gluon-quark vertex (Fig. 24a). The remaining terms result from substitutions (A.2), and represent new four-quanta interactions containing instantaneous fermion and gluon propagators (Fig. 24b). All terms conserve total three-momentum $\underline{k} = (k^+,\vec{k}_\perp)$, because of the integral over $\underline{x}$ in V. Furthermore, all Fock states other than the vacuum have total $k^+ > 0$, since each individual bare quantum has $k^+ > 0$ (Eq.(A.3)). Consequently the Fock state vacuum must be an eigenstate of V and therefore an eigenstate of the full light-cone Hamiltonian.

Light-Cone Perturbation Theory

We define light-cone Green's functions to be the probability amplitude that a state starting in Fock state $|i>$ ends up in Fock state

$|f\rangle$ a (light-cone) time τ later

$$\langle f|i\rangle \; G(f,i;\tau) \equiv \langle f|\, e^{-iH_{LC}\tau/2}|i\rangle$$
$$= i\int\frac{d\varepsilon}{2\pi}\, e^{-i\varepsilon\tau/2}\, G(f,i;\varepsilon)\langle f|i\rangle \qquad (A.8)$$

where Fourier transform $G(f,i;\varepsilon)$ can be written

$$\langle f|i\rangle G(f,i;\varepsilon) = \langle f|\frac{1}{\varepsilon-H_{LC}+i0_+}|i\rangle$$
$$= \langle f|\frac{1}{\varepsilon-H_0+i0_+} + \frac{1}{\varepsilon-H_0+i0_+}\,V\,\frac{1}{\varepsilon-H_0+i0_+} \qquad (A.9)$$
$$+ \frac{1}{\varepsilon-H_0+i0_+}\,V\,\frac{1}{\varepsilon-H_0+i0_+}\,V\,\frac{1}{\varepsilon-H_0+i0_+} + \ldots|i\rangle$$

The rules for τ-ordered perturbation theory follow immediately from the pansion in (A.9) when $(\varepsilon-H_0)^{-1}$ is replaced by its spectral decomposition terms of Fock states:

$$\frac{1}{\varepsilon-H_0+i0_+} = \sum_{n,\lambda_i}\int\tilde{\Pi}\frac{dk_i^+ d^2k_{\perp i}}{16\pi^3 k_i^+}\;\frac{|n:\,\underline{k}_i,\lambda_i\rangle\langle n:\,\underline{k}_i,\lambda_i|}{\varepsilon-\sum_i(k^2+m^2)_i/k_i^+ + i0_+} \qquad (A.10)$$

ere in (A.9) the sum becomes a sum over all states n intermediate between interactions. To calculate $G(f,i;\varepsilon)$ perturbatively then, all τ-ordered diagrams (i.e. all orderings of the vertices, as in Fig. 25) must be considered, the contribution from each graph computed according to the following rules:

1) Assign a momentum k^μ to each line such that the total $k^+,k_\perp$ are conserved at each vertex, and such that $k^2=m^2$ — i.e. $k^-=(k^2+m^2)/k^+$. With fermions associate an on-shell spinor (from Eq.(A.2))

$$u(\underline{k},\lambda) = \frac{1}{\sqrt{k^+}}\,(k^+ + \beta m + \vec{\alpha}_\perp \cdot \vec{k}_\perp) \begin{cases} \chi(\uparrow) & \lambda = \uparrow \\ \chi(\downarrow) & \lambda = \downarrow \end{cases}$$

or

$$v(\underline{k},\lambda) = \frac{1}{\sqrt{k^+}}(k^+ - \beta m + \vec{\alpha}_\perp \cdot \vec{k}_\perp) \begin{cases} \chi(\downarrow) & \lambda = \uparrow \\ \chi(\uparrow) & \lambda = \downarrow \end{cases}$$

where $\chi(\uparrow) = \frac{1}{\sqrt{2}}\,(1,0,1,0)^T$ and $\chi(\downarrow) = \frac{1}{\sqrt{2}}\,(0,1,0,-1)^T$. For gluon lines, assign a polarization vector $\varepsilon^\mu = (0, \frac{2\vec{\varepsilon}_\perp \cdot \vec{k}_\perp}{k^+}, \vec{\varepsilon}_\perp)$ where $\vec{\varepsilon}_\perp(\uparrow) = -\frac{1}{\sqrt{2}}(1,i)$ and $\vec{\varepsilon}_\perp(\downarrow) = \frac{1}{\sqrt{2}}(1,-i)$.

2) Include a factor $\theta(k^+)/k^+$ for each internal line.

3) For each vertex include factors as illustrated in Fig. 26. To convert incoming into outgoing lines or vice versa replace

$$u \leftrightarrow v \qquad \bar{u} \leftrightarrow -\bar{v} \qquad \varepsilon \leftrightarrow \varepsilon^*$$

in any of these vertices.

4) For each intermediate state (e.g., as indicated by dashed lines in Fig. 25) there is a factor

$$\frac{1}{\varepsilon - \sum_{\text{interm}} k^- + i0_+}$$

where ε is the incident P^-, and the sum is over all particles in the intermediate state.

5) Integrate $\int \frac{d\,k^+ d^2k_\perp}{16\pi^3}$ over each independent $\underline{k}$, and sum over internal helicities and colors.

6) Include a factor -1 for each closed fermion loop, for each fermion line that both begins and ends in the initial state (i.e. $\bar{v}$....u), and for each diagram in which fermion lines are interchanged in either of the initial or final states.

As an illustration, the second diagram in Fig. 25 contributes

$$\frac{1}{\varepsilon - \sum_{i=b,d}\left[\frac{k_\perp^2+m^2}{k^+}\right]_i}\,\frac{\theta(k_a^+-k_b^+)}{k_a^+-k_b^+}\,\frac{g^2\sum_\lambda \bar{u}(b)\not{\epsilon}^*(\underline{k}_a-\underline{k}_b,\lambda)u(a)\bar{u}(d)\not{\epsilon}(\underline{k}_a-\underline{k}_b,\lambda)u(c)}{\varepsilon - \sum_{i=b,c}\left[\frac{k_\perp^2+m^2}{k^+}\right]_i - \frac{(k_{\perp a}-k_{\perp b})^2}{k_a^+-k_b^+}}\,\frac{1}{\varepsilon - \sum_{i=a,c}\left[\frac{k_\perp^2+m^2}{k^+}\right]_i}$$

(times a color factor) to the $q\bar{q}\to q\bar{q}$ Green's function. [The vertices for quarks and gluons of definite helicity have very simple expressions in terms of the momenta of the particles — see for example Refs. 1,33]. These same rules apply for scattering amplitudes, but with propagators omitted for external lines, and with $\varepsilon = P^-$ of the initial (and final) states.

Finally, notice that this quantization procedure and perturbation theory (graph by graph) are manifestly invariant under a large class of orentz transformations:

) boosts along the 3-direction — i.e. $p^+\to Kp^+$, $p^-\to K^{-1}p^-$, $p_\perp\to p_\perp$ for each momentum;

b) transverse boosts — i.e. $p^+\to p^+$, $p^-\to p^- + 2p_\perp\cdot Q_\perp + p^+Q_\perp^2$, $p_\perp\to p_\perp + p^+Q_\perp$ for each momentum ($Q_\perp$ like K is dimensionless);

c) rotations about the 3-direction

It is these invariances which lead to the frame independence of the Fock state wave functions, as discussed in Section 2.A.

Appendix B — Which α_s? [34]

A major ambiguity in the interpretation of perturbative expansions in QCD is in the choice of an expansion parameter. In general QCD predictions for some measurable quantity ρ have the form

$$\rho = C_0\alpha_s(M)\ \{1+ C_1(M)\ \frac{\alpha_s(M)}{\pi} + C_2(M)\ \frac{\alpha_s(M)}{\pi^2} + \ldots\}\ . \qquad (B.1)$$

The coefficients $C_i(M)$ depend upon both the exact definition of the running coupling constant $\alpha_s(M)$ (i.e. the 'scheme'), and upon the choice of scale M. When working to all orders in $\alpha_s(M)$ the choice of scheme and scale is irrelevant; the coefficients $C_i(M)$ are defined so that ρ is the same for all choices. However this freedom can be a serious source of confusion in finite order analyses. Indeed when working to first order, one can set $C_1(M)$ to any value simply by redefining α_s or by changing M. This coefficient seems meaningless here. In particular it seems to give no indication of the convergence of the expansion.

This is in marked contrast with the situation in low energy QED, where for example the electron anomaly has a very convergent expansion,

$$a_e = \frac{g_e-2}{2} = \frac{\alpha}{2\pi}\ [1 - 0.656\left(\frac{\alpha}{\pi}\right)^2 + 2.352\left(\frac{\alpha}{\pi}\right)^3 + \ldots] \qquad (B.2)$$

while the expansion for orthopositronium decay is much less convergent:

$$\Gamma_{o\text{-}Ps} = \Gamma_0(1 - 10.3\ \frac{\alpha}{\pi} + \ldots) \qquad (B.3)$$

The difference in convergence rate here is not an artifact due to a bad choice of scheme or scale; the coefficients in these expansions should not be absorbed into a redefinition of $\alpha(M)$ since the running coupling constant

for QED doesn't run below e^+e^- threshold.

QED

In QED the running coupling constant has an obvious definition ($Q^2 = -q^2$):

$$\alpha_0 d_{\mu\nu}(q) \equiv \alpha(Q) \frac{-g^{\mu\nu} + q^\mu q^\nu/q^2}{q^2 + i\varepsilon} \qquad (B.4)$$

where α_0 is the bare coupling, and $d^{\mu\nu}$ the unrenormalized photon propagator (in Landau gauge). The entire vacuum polarization correction is absorbed into $\alpha(Q)$. Since the only true ultraviolet divergences in the theory are associated with vacuum polarization, it is only these corrections which make the coupling constant run.

Given the definition, we need only determine the appropriate scale (or scales) Q for a given process. The most naive procedure is simply to use the full propagator (Eq.(B.4)) for each photon in any given diagram.[35] For example, we can replace α by $\alpha(Q)$ (with $Q^2 = -q^2$) before integrating over q in the leading diagram for the muon anomaly (Fig. 27a). All vacuum polarization insertions are automatically included. Unfortunately the loop integration is then quite cumbersome. However, by the mean value theorem there must be some scale $Q^* \sim m_\mu$ for which the exact result is

$$a_\mu^{VP} = \frac{\alpha(Q^*)}{2\pi} \qquad (B.5a)$$

where from Eq.(B.2)

$$\alpha(Q) = \frac{\alpha}{1 - \frac{\alpha}{\pi}\left(\frac{2}{3}\ell n\frac{Q}{m_e} - \frac{5}{3}\right) - \left(\frac{\alpha}{\pi}\right)^2\left(\frac{1}{2}\ell n\frac{Q}{m_e} + \zeta(3) - \frac{25}{24}\right) - \ldots} \qquad \text{(B.5b)}$$

(For simplicity we are neglecting muon loops and factors of order m_e/m_μ or less in $\alpha(Q)$). Scale Q^* can then be determined order by order in perturbation theory by expanding (B.5) in powers of α and adjusting the coefficients to agree with results obtained from vacuum polarization insertions in the basic diagram. For example the lowest order electron loop (Fig. 27b) contributes

$$A_{VP}\frac{\alpha}{\pi}a_\mu^o = \left(\frac{2}{3}\ell n\frac{m_\mu}{m_e} - \frac{25}{18}\right)\frac{\alpha}{\pi}a_\mu^o$$

which from Eq. (B.5) must equal

$$\left(\frac{2}{3}\ell n\frac{Q^*}{m_e} - \frac{5}{3}\right)\frac{\alpha}{\pi}a_\mu^o$$

Thus we have $Q^* = m_\mu e^{5/12}$ in leading order. With this procedure, the muon anomaly has the same expansion to first order as the electron anomaly Eq.(B.2)) — i.e. to this order we are replacing

$$a_\mu = \frac{\alpha}{2\pi}\left(1 + \frac{\alpha}{\pi}\left(A_{VP} - 0.656\right) + \ldots\right)$$

by

$$a_\mu = \frac{\alpha(Q^*)}{2\pi}\left(1 - \frac{\alpha(Q^*)}{\pi}0.656 + \ldots\right) \qquad \text{(B.7a)}$$

where

$$\alpha(Q^*) \simeq \frac{\alpha}{1 - \frac{\alpha}{\pi}A_{VP}} \qquad \text{(B.7b)}$$

Intuitively this is reasonable since if a single insertion gives $\frac{\alpha}{\pi}A_{VP}$, a double insertion will give roughly $\left(\frac{\alpha}{\pi}A_{VP}\right)^2$, and so on. Thus the electrons modify only the charge and not the physical expansion of a_μ in this order. Of course this is no longer the case in higher orders, when 'light-by-light' diagrams (Fig. 27c) and others like them appear.

The optimal scale Q^* is refined by higher order corrections — $Q^* = m_\mu e^{5/12}\left(1 + 1.14\,\frac{\alpha}{\pi} + \ldots\right)$ — but its expansion is obviously far more convergent than the original expansion for a_μ. Also this expansion is unique. For example, including the $-.656\,\frac{\alpha}{\pi}$ from (B.7a) with the $A_{VP}\,\frac{\alpha}{\pi}$ in $\alpha(Q^*)$ (Eq.(B.7b)) would wreak havoc with the next-to-leading logarithms of m_μ/m_e in higher orders; there is no reason to expect that the $-.656\,\frac{\alpha}{\pi}$ is part of an approximately geometric series of contributions, unlike the vacuum polarization corrections which must be (for renormalizability). Finally when there are several photons in a diagram, each will usually have its own scale (determined as above). There is no reason for all running couplings to have the same scale.

QCD

We would like now to carry these ideas over to QCD. However we immediately encounter a difficulty. In QCD, the charge is renormalized not only by vacuum polarization but by parts of the vertex and fermion self energy corrections as well. It seems generally impossible to separate these latter corrections into a more or less process independent piece which renormalizes the charge, and a process dependent, ultraviolet-finite remainder; but for processes having no tri-gluon couplings in

lowest order there is a way, and these include almost all phenomenologically relevant processes in QCD.

For such processes the only ultraviolet divergent fermion loops in first order are insertions in the gluon propagators. As for the muon anomaly, the only function of these light-fermion insertions is to renormalize the coupling; all such terms should be completely absorbed into a redefinition of α_s (or of its scale). Unfortunately it is less clear which of the gluonic corrections should also be included. However only terms proportional to $\beta_0 = 11 - \frac{2}{3}n_f$ can be absorbed in this order. So we can use the light-quark loops as a probe, absorbing not just the quark polarization contributions but the implied gluonic corrections required to give the $11 - \frac{2}{3}n_f$ dependence — e.g. if the $A_{VP}n_f$ term is due to n_f quark insertions, we take

$$\begin{aligned} \rho &= \alpha_{\overline{MS}}(Q)\ \{1 + \frac{\alpha_{\overline{MS}}}{\pi}\ (A_{VP}n_f + B) + \ldots\} \\ &= \alpha_{\overline{MS}}(Q)\ \{1 + \frac{\alpha_{\overline{MS}}}{\pi}\ (-\frac{3}{2}\beta_0 A_{VP} + \frac{33}{2}\ A_{VP} + B) + \ldots\} \\ &\to \tilde{\alpha}(Q)\quad \{\ 1 + \frac{\tilde{\alpha}}{\pi}\ (\frac{33}{2}A_{VP} + B) + \ldots\} \end{aligned} \tag{B.8a}$$

where as in (B.7b)

$$\begin{aligned} \tilde{\alpha}(Q) &\equiv \frac{\alpha_{\overline{MS}}(Q)}{1 + \beta_{o2}\frac{3}{2}A_{VP}\frac{\alpha_{\overline{MS}}(Q)}{\pi}} \\ &= \alpha_{\overline{MS}}(Q\ \exp(3A_{VP})) \end{aligned} \tag{B.8b}$$

(The last line in (B.8b) is a consequence of the fact that all definitions of α_s have the same functional form in two loops, one definition differing from the other only by a scale factor).[36] The term $\frac{33}{2}\ A_{VP}$ in (B.8a) in

effect removes that part of the constant B which renormalizes the charge.

This procedure determines the natural expansion parameter $\tilde{\alpha}(Q)$ for the majority of interesting processes in QCD. Coupling $\tilde{\alpha}$ is gauge invariant, and independent of the scheme or scale chosen for the original calculation (here we assume) $\overline{\text{MS}}$). Viewed another way, given a scheme ($\overline{\text{MS}}$, MS, MOM, ...) this procedure automatically determines the optimal scale, $Q^* = Q \exp(3 A_{VP})$ (where A_{VP} and therefore Q^* obviously depend upon the scheme chosen).

Processes with tri-gluon couplings in lowest order are more difficult to analyze because in first order quark loops appear not only as propagator insertions, but also in the radiative corrections to the tri-gluon vertex. Again it is hard to separate the divergent part of the vertex (which renormalizes α) from the finite part in any unique and general fashion. Such processes are discussed elsewhere.[34]

To illustrate this procedure and to explore its implications, we examine briefly a number of well know predictions of QCD:

<u>$e^+e^- \to$ hadrons</u> — The ratio of the total cross section into hadrons to the cross section for $e^+e^- \to \mu^+\mu^-$ is ($s = E^2$)[37]

$$R(E) = 3 \sum_q e_q^2 \{1 + \frac{\alpha_{\overline{\text{MS}}}(E)}{\pi} + \frac{\alpha_{\overline{\text{MS}}}}{\pi^2} (1.98 - 0.115\, n_f) + \ldots\}$$

$$\to 3 \sum_q e_q^2 \{1 + \frac{\tilde{\alpha}(E)}{\pi} + \frac{\tilde{\alpha}^2(E)}{\pi^2} 0.08 + \ldots\}$$

where $\tilde{\alpha}(E) = \alpha_{\overline{\text{MS}}}(0.71E)$ for four flavors.

<u>Deep Inelastic Scattering</u> — The momenta of the non-singlet structure

function $F_2(x,Q^2)$ have an evolution equation[38]

$$Q^2\frac{d}{dQ^2}\ell n M_n(Q^2) = -\frac{\gamma_n^{(o)}}{8\pi}\alpha_{\overline{MS}}(Q)\left\{1+\frac{\alpha_{\overline{MS}}}{4\pi}\frac{2\beta_o B_n+\gamma_n^{(1)}}{\gamma_n^{(o)}}\right\}$$

$$\to -\frac{\gamma_n^{(o)}}{\pi}\tilde{\alpha}_n(Q)\left\{1-\frac{\tilde{\alpha}_n(Q)}{\pi}C_n+\ldots\right\}$$

where for example

$$\tilde{\alpha}_2(Q) = \alpha_{\overline{MS}}(0.48Q)\ C_2 = .27 \quad \text{for } n=2$$

$$\tilde{\alpha}_{10}(Q) = \alpha_{\overline{MS}}(0.21Q)\ C_{10}=1.1 \quad \text{for } n=10\ .$$

For n very large, the effective scale here becomes $Q^* \sim Q/\sqrt{n}$ which is exactly what was found in Ref. 39 by a detailed study of the kinematics of deep inelastic scattering.

<u>η_c Decay</u> — The ratio of the η_c width into hadron to that into $\gamma\gamma$ is (Eq. 4.11)

$$\frac{\Gamma(\eta_c\to\text{hadrons})}{\Gamma(\eta_c\to\gamma\gamma)} = C_o\,\alpha_{\overline{MS}}^2(M\eta_c)\left\{1+\frac{\alpha_{\overline{MS}}}{\pi}(17.13-\frac{8}{9}n_f)+\ldots\right\}$$

$$\to C_o\,\tilde{\alpha}^2(M\eta_c)\left\{1+\frac{\alpha(M\eta_c)}{\pi}2.46+\ldots\right\}$$

where here $\tilde{\alpha}(M) = \alpha_{\overline{MS}}(0.26\ M)$ for three flavors.

<u>T Decay</u> — The ratio of the hadronic to the leptonic widths of the T (Eq.(4.9)) can be rewritten

$$\frac{\Gamma(T\to\text{hadrons})}{\Gamma(T\to\mu^+\mu^-)} = C_o\tilde{\alpha}^3(M_T)\left\{1-\frac{\tilde{\alpha}(M_T)}{\pi}14.0+\ldots\right\}$$

where $\tilde{\alpha}(M_\Upsilon) = \alpha_{\overline{MS}}(0.157\ M_\Upsilon)$. Thus the rate into gluons has a large negative correction with this physical definition of α_s, just as do the rates for $\Upsilon \to \gamma\gamma\gamma$ and for o-Ps $\to \gamma\gamma\gamma$, both of which are scheme-scale independent. Such a correction implies large, positive terms in higher orders, and in fact these are necessary if we are to fit the data — otherwise the ratio becomes negative for large $\tilde{\alpha}$. We can still do a fit if we replace the term in brackets by $\{1 - \frac{\tilde{\alpha}}{\pi}7\}^2$ in which case we obtain $\Lambda_{\overline{MS}} \sim 140$-$230$ MeV, which is surprisingly close to our original estimate (Eq.(4.10)) from this process. This last procedure might be justified because more than half the negative coefficient comes from a single diagram (Fig. 28) and this may in effect simply modify $\psi(0)$. Further study is clearly necessary, though $\Lambda_{\overline{MS}} \sim$ 100-200 MeV seems very likely.

References and Footnotes

1. S. J. Brodsky and G. P. Lepage, in 'Quantum Chromodynamics' the proceedings of the 1978 La Jolla Institute Summer Workshop, W. Frazer and F. Henyey (eds.), AIP, 1979; Phys. Lett. 87B, 359 (1979); Phys. Rev. Lett. 43, 545 (1979), Erratum ibid 43, 1625 (1979); 'Quantum Chromodynamics' in the proceedings of the 1979 Summer Institute on Particle Physics at SLAC, Stanford, California; Phys. Rev. D22, 2157 (1980); S. J. Brodsky, T. Huang and G. P. Lepage, in preparation.
2. Many early applications of these ideas are made by S. D. Drell, D. Levy and T. M. Yan, Phys. Rev. 187, 2159 (1969); D1, 1617 (1970); D1, 1035 (1970); J. Kogut and L. Susskind, Phys. Rep. 8C, 75 (1973). See also R. P. Feynman, Photon-Hadron Interactions (Benjamin, 1972).
3. Modern analyses of exclusive processes are discussed in Ref. 1. See also V. L. Chernyak and A. R. Vhitaishii , JETP Lett. 25, 11 (1977); G. R. Farrar and D. R. Jackson, Phys. Rev. Lett. 43, 246 (1979); A. V. Efremov and A. V. Radyushkin, Rev. Nuovo Cim. 3, 1(1980); Phys. Lett. 94B, 245 (1980); G. Parisi, Phys. Lett. 43, 246 (1979); A. Duncan and A. H. Mueller, Phys. Lett. 93B, 119 (1980); A. H. Mueller, Phys. Rep. 73, 237 (1981).
4. Here $V_{eff} = K/\sqrt{x(1-x)y(1-y)}$ where K is the irreducible scattering amplitude. Helicity dependence is implicit here.
5. The approach here is similar in spirit to that of J. Kogut and L. Susskind, Phys. Rev. D9, 697 (1973).

6. Such regulators exist for QCD (see L. D. Faddeev and A. A. Shavnov, Gauge Fields (Benjamin, 1980)), but they are cumbersome to say the least. Similar results can be obtained more easily by dimensionally regulating the $k_\perp$ integrations and setting $\mu = \Lambda$, the cut-off desired. The former regulator is more intuitive, however, and we adopt it for our discussions here.

7. Fermion polarization sums must be similarly regulated.

8. S. D. Drell and T. M. Yan, Phys. Rev. Lett. 24, 181 (1970); G. West, Phys. Rev. Lett. 24, 1206 (1970).

9. F. Ezawa, Nuovo Cim. 23A, 271 (1974); G. R. Farrar and D. R. Jackson, Phys. Rev. Lett. 35, 1416 (1975); A. I. Vainshtain and V. I. Zakharov, Phys. Lett. 72B, 368 (1978).

10. Examples of this have been given by A. De Rujula and F. Martin, MIT preprint CTP 851 (1980).

11. They also show that $F_{\pi\gamma}(Q^2) \sim 1/Q^2$ for very large Q^2, in complete disagreement with a naive application of PCAC. One must take care in assuming pion pole dominance of axial vector amplitudes involving a large energy scale.

12. The $k_\perp$ integration is easily performed for $q_\perp \to 0$ by changing integration variables to $\ell_\perp = k_\perp + (1-x)q_\perp$, and expanding the wave function $\psi(x,\ell_\perp-(1-x)q_\perp) = \psi(x,\ell_\perp)-(1-x)q_\perp \cdot \frac{\partial}{\partial \ell_\perp}\psi(x,\ell_\perp)$. The angular integration kills the first term in the expansion of ψ, while the second term reduces to $\int \ell_\perp^2 \frac{\partial}{\partial \ell_\perp^2}\psi(x,\ell_\perp)$ which leads immediately to the final result.

13. Our analysis is mathematically similar to Jackiw's analysis of the axial vector anomaly using 'point splitting techniques' (see S. Treiman, R. Jackiw and D. Gross, Lectures on Current Algebra and its Applications, Princeton University Press (Princeton, 1972)). Of course PCAC provides the link between his analysis of the axial vector amplitude and our direct analysis of $\pi \to \gamma\gamma$.

14. By 'radius' we mean the slope of the form factor near $Q^2 \simeq 0$: $F_\pi(Q^2) = 1 - \frac{Q^2}{6} R_\pi^2$.

15. This gauge invariant amplitude is defined in other gauges by (3.2b) but with a path order 'string' operator $P \exp(\int_0^1 ds\ ig\ A(sz)\cdot z)$ between the $\bar{\psi}$ and ψ. The line integral vanishes in light cone gauge because $A\cdot z = A^+ z^- = 0$. This all orders definition of ϕ uniquely fixes the definition of T_H which must itself then be gauge invariant.

16. For example, the full unrenormalized quark propagator has the form $d_F(\Lambda^2, Q^2, \alpha_s^{(\Lambda)})/q$ as $Q^2 = -q^2 \to \infty$, where d_F has no mass singularities (for $A^+ = 0$ gauge) and is therefore independent of masses in this limit. Similarly $Z_2^{(\Lambda)}/Z_2^{(Q)} = \exp -\int_Q^\Lambda \frac{d\Lambda^2}{\Lambda^2} \gamma_F(\alpha(\Lambda))$ is free of mass singularities. Thus the product $Z_2^{(Q)}\ d_F(\Lambda^2, Q^2, \alpha_s(\Lambda))/Z_2^{(\Lambda)}$ is independent of cut-off Λ and all masses for large Q^2, and must therefore be a function only of $\alpha_s(Q)$ — there is no other dimensionless function of Q. Thus we have $d_F = Z_2^{(\Lambda)}/Z_2^{(Q)}(1 + O(\alpha_s(Q))$ as required.

17. This amplitude is also given by (3.24) in gauges other than light-cone gauge, but with $i\partial^+ \to i\partial^+ - gA^+$.

18. S. J. Brodsky, Y. Frishman, G. P. Lepage and C. Sachrajda, Phys. Lett. 91B, 239 (1980); see also Refs. 1 and 3.

19. The importance of these Sudakov corrections for form factors was emphasized by Duncan and Mueller, Ref. 3. See also Ref. 1.

20. W. Buchmuller and S. H. Tye, Phys. Rev. D24, 132 (1981), and references therein.

21. We are simplifying matters slightly here, and later. The coupling to gauge fields could also have the form $g^2\vec{A}^2$, and could proceed through multipole couplings other than E1. The E1 coupling we assume here is typical of all the couplings, and frequently dominant among them.

22. W. Buchmuller, J. Ng and S. H. Tye, Fermilab preprint PUB-81/4.

23. In general, each additional $Q\bar{Q}$ interaction during the gluon propagation results in a factor of order $\int d^3k\, V(\ell - k)(\Delta\varepsilon - k^2/2m)^{-1}$ $\sim \langle V\rangle/\Delta\varepsilon \sim 1$, and thus diagrams with any number of interactions contribute. This sort of 'false expansion' in powers of V is nicely explained for QED in D. R. Yennie, in Lectures on Strong and Electromagnetic Interactions, Brandeis Summer Institute, Vol I(1963). For a discussion of a quark in a uniform chromomagnetic field, see J. Sapirstein, Phys. Rev. D20, 3246 (1979).

24. This result follows in close analogy to the analysis of orthopositronium decay: A. Ore and J. L. Powell, Phys. Rev. 75, 1696 (1949).

25. This general result is obviously correct in perturbation theory — see I. J. Muzinick and F. E. Paige, Phys. Rev. D21, 1151 (1980).

26. P. B. Mackenzie and G. P. Lepage, Phys. Rev. Lett. 47, 1244 (1981).

27. R. Barbieri et al, Nucl. Phys. B154, 535 (1979).

28. Results similar to those presented here have also been obtained by I. Hinchliffe and J. Sheiman, private communication.

29. R. Barbieri et al., Phys. Lett. 61B, 465 (1976); Phys. Lett. 95B, 93 (1980).

30. K. Gottfried, Phys. Rev. Lett. 40, 598 (1978); G. Bhanot et al, Nucl. Phys. B155, 208 (1979); M. E. Peskin, Nucl. Phys. B156, 365 (1979); G. Bhanot and M. E. Peskin, Nucl. Phys. B156, 391 (1979); T. M. Yan, Phys. Rev. D22, 1652 (1980); K. Shizuya, Phys. Rev. D23, 1180 (1981).

31. Y. P. Kuang and T. M. Yan, Cornell preprint CLNS 81/495; see also T. M. Yan, Ref. 30.

32. M. G. D. Gilchriese, in the Proceedings of the SLAC Summer Institute on Particle Physics (1981) (also Cornell Preprint CLNS-81/518).

33. The light-cone quantization of QED is described in J. B. Kogut and D. E. Soper, Phys. Rev. D1, 2901 (1970); J. B. Bjorken, J. B. Kogut and D. E. Soper, Phys. Rev. D3, 1382 (1971). See also S. Weinberg, Phys. Rev. 150; L. Susskind and G. Frye , Phys. Rev. 165, 1535 (1968); S. D. Drell, D. Levy and T. M. Yan, Ref. 2.

34. S. J. Brodsky, G. P. Lepage, and P. B. Mackenzie, in preparation.

35. The Landau singularity (where $\alpha(Q) \to \infty$) does not occur when the ultraviolet divergences are regulated using the Pauli-Villars method, provided the cut-off is finite with $\Lambda << e^{3\pi/2\alpha}m$. This is because the running coupling constant stops running for $Q^2 \gtrsim \Lambda^2$, and therefore

does not diverge as $Q^2 \to \infty$. As always, keeping Λ finite in no way affects the predictions of the theory so long as Λ is much larger than all important energy scales.

36. To two loops, all definitions of α_s have the form $\alpha_s(Q) = 4\pi/(\beta_0 \ell n\, Q^2/\Lambda^2 + \frac{\beta_1}{\beta_0} \ell n \ell n\, Q^2/\Lambda^2)$, where $\beta_0 = 11\text{-}2\, n_f/3$, $\beta_1 = 102 - 38\, n_f/3$.

37. M. Dine and J. Sapirstein, Phys. Rev. Lett. 43, 668 (1979).

38. For a review see A. J. Buras, Rev. Mod. Phys. 52, 1 (1980).

39. S. J. Brodsky and G. P. Lepage, Ref. 1 — 1979 SLAC Summer Institute. See also D. Amati et al., Nucl. Phys. B173, 429 (1980).

Figure Captions

1. Perturbative contributions to the pion's $q\bar{q}q\bar{q}g$ wave function. Contributions of type b) correspond to creation of $q\bar{q}g$ from the vacuum, and therefore do not appear in equal-τ wave functions.
2. Coupled eigenvalue equations for the Fock state wave functions of a pion.

3a) Bound state equation for the $e\bar{e}$ Fock state wave function of positronium

b) The two-particle irreducible potential.

4. Diagrams having similar behavior to wave functions for large $k_\perp$.
5. Diagrams contributing to the pion form factor.
6. Diagrams contributing to the structure functions for deep inelastic scattering.
7. Amplitudes whose behavior is similar to that of wave functions for $x \to 1$
8. The π-γ transition form factor.
9. Diagrams contributing to $F_{\pi\gamma}$ as $q_\perp \to 0$.
10. The contribution to $F_{\pi\gamma}$ from the diagram in Fig. 9b.
11. The two-particle irreducible amplitude for $\gamma^* + q\bar{q} \to q\bar{q}$, in the pion form factor.
12. The $q\bar{q}$ component of the pion form factor.
13. The unrenormalized hard scattering amplitudes for F_π.
14. Vertex and propagator corrections for F_π.
15. Hard scattering amplitudes for $\gamma^* + q\bar{q}g \to q\bar{q}$.
16. The $q\bar{q}$ wave function of the pion for $q_\perp^2 = Q^2$ large.

17 a) Diagram contributing to $\pi\pi$ elastic scattering.

b) Hard scattering amplitude coming from a) when $k_a^2 \sim r_\perp^2, q_\perp^2$.

18. Various models (see Ref. 20) for the $Q\bar{Q}$ potential, with the mean radii of the T, T', ψ, ψ', ... as indicated. The curves correspond to 1) a power law potential, 2) a refined Richardson potential, 3) a logarithmic potential, and 4) a linear plus Coulomb potential.

19. Wave functions for higher Fock states in $Q\bar{Q}$ mesons.

20 a) Lowest order diagrams contributing to the hyperfine splitting in $Q\bar{Q}$ mesons.

b) Diagrams which are typical of the infinity of diagrams contributing to the $O(\alpha_s)$ corrections to the hyperfine splitting.

21 a) Leading order diagram for $T \to$ gluons ($\to$ hadrons).

b) Contribution to $T \to$ gluons from $Q\bar{Q}g$ Fock states.

c) Contribution from $Q\bar{Q}g$ states to the decay of p-states.

d) Typical diagram contributing to p-state decays in leading order.

22. QED radiative decays of the ψ'.

23. QCD radiative decays of the T'.

24. Interaction vertices for QCD.

25. Diagrams contributing to the $qq \to qq$ Green's function in LCPTh.

26. Graph rules for QCD vertices in LCPTh.

27. Diagrams for the muon anomaly.

28. Diagram contributing to $T \to ggg$.

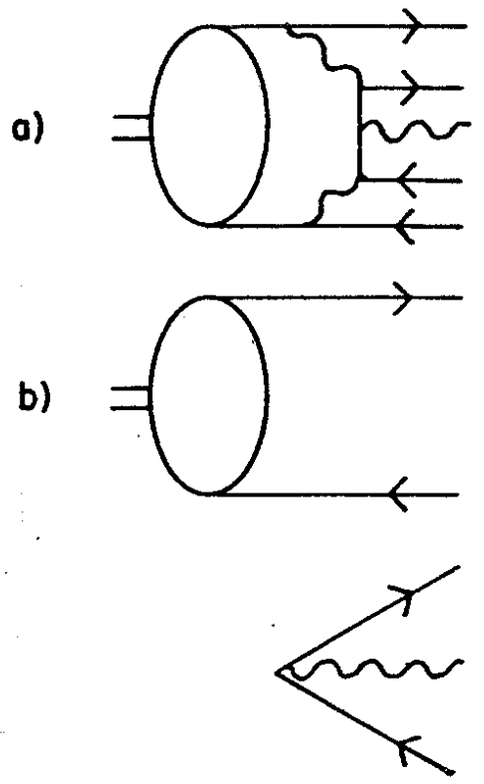

FIG. 1

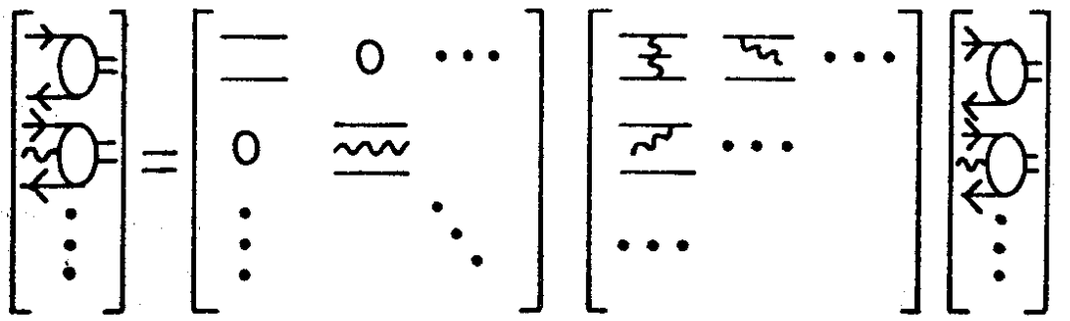

FIG. 2

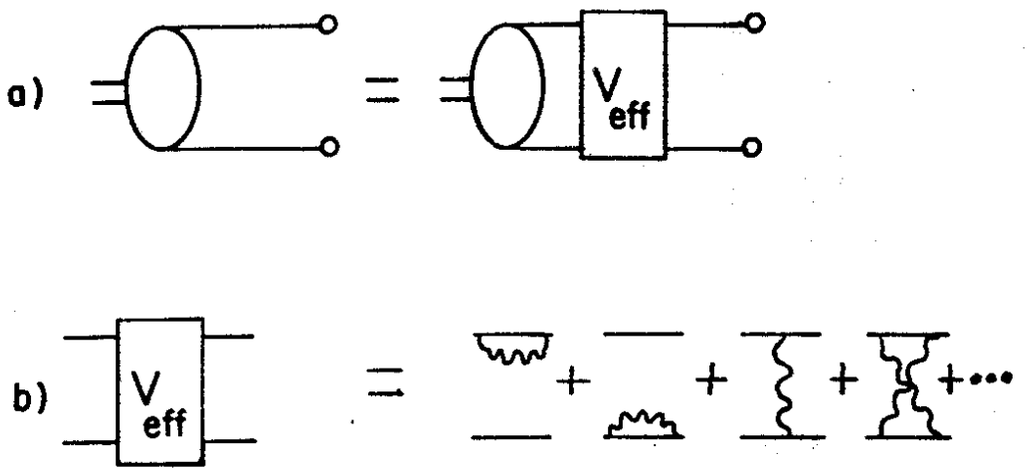

FIG. 3

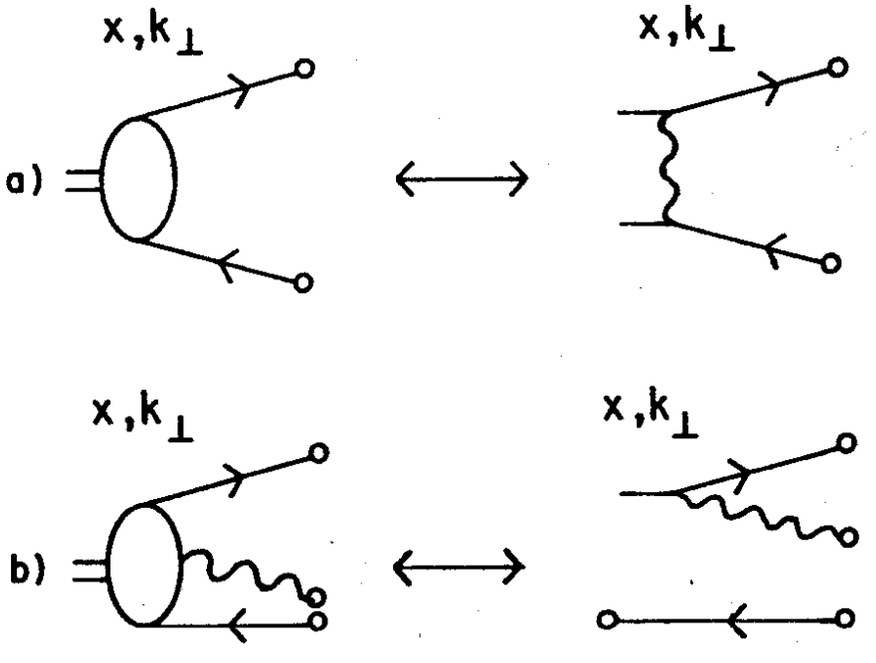

FIG. 4

0771281

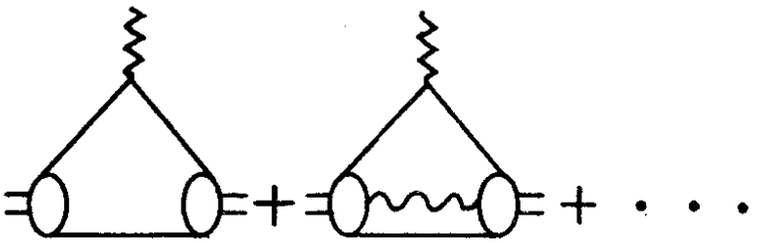

FIG.5

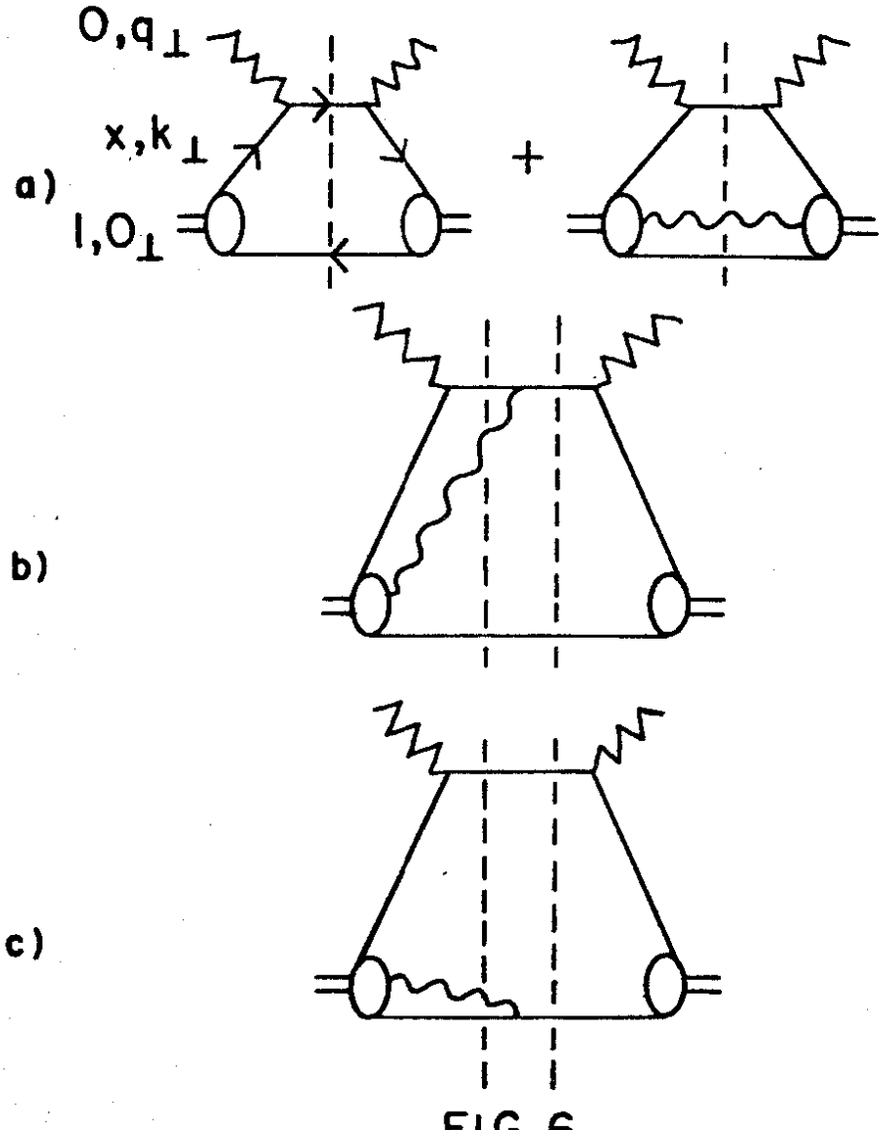

FIG.6

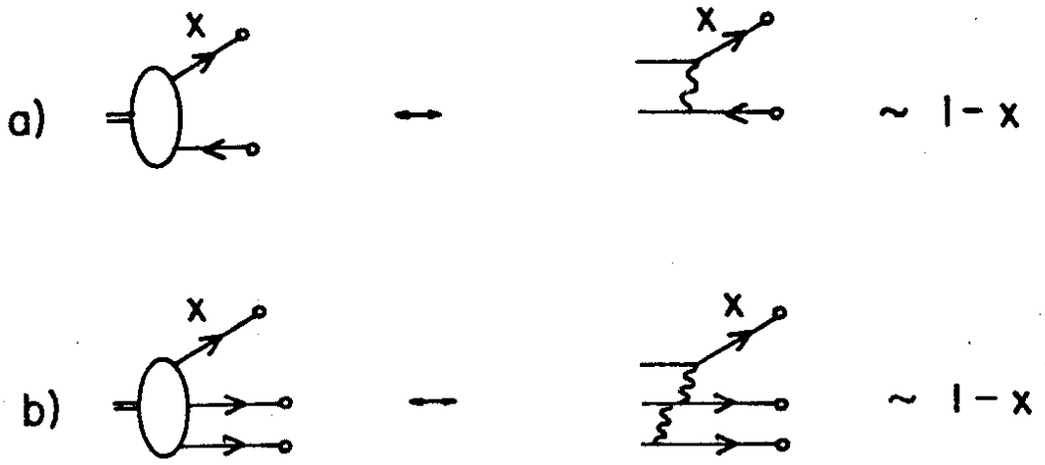

FIG. 7

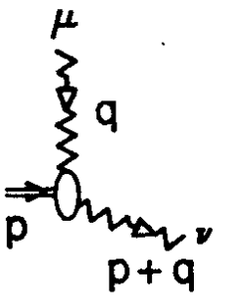

FIG. 8

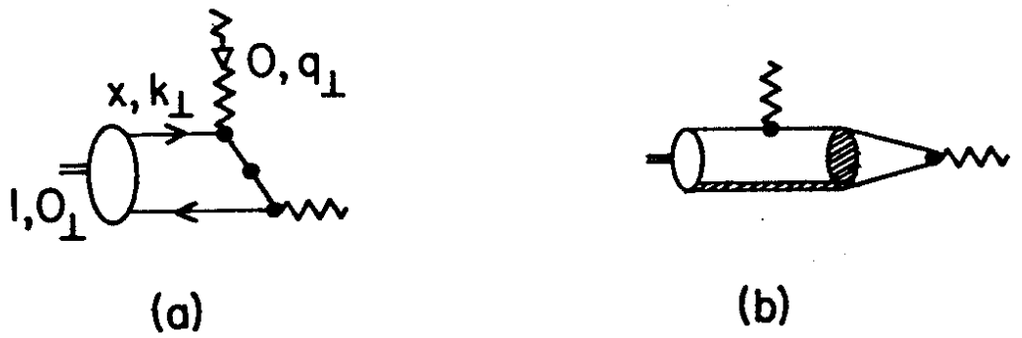

FIG. 9

0771281

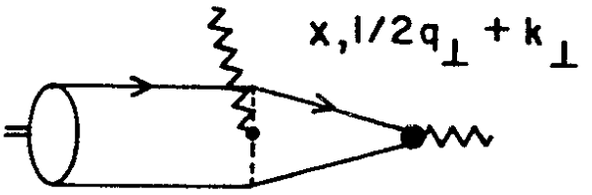

FIG. 10

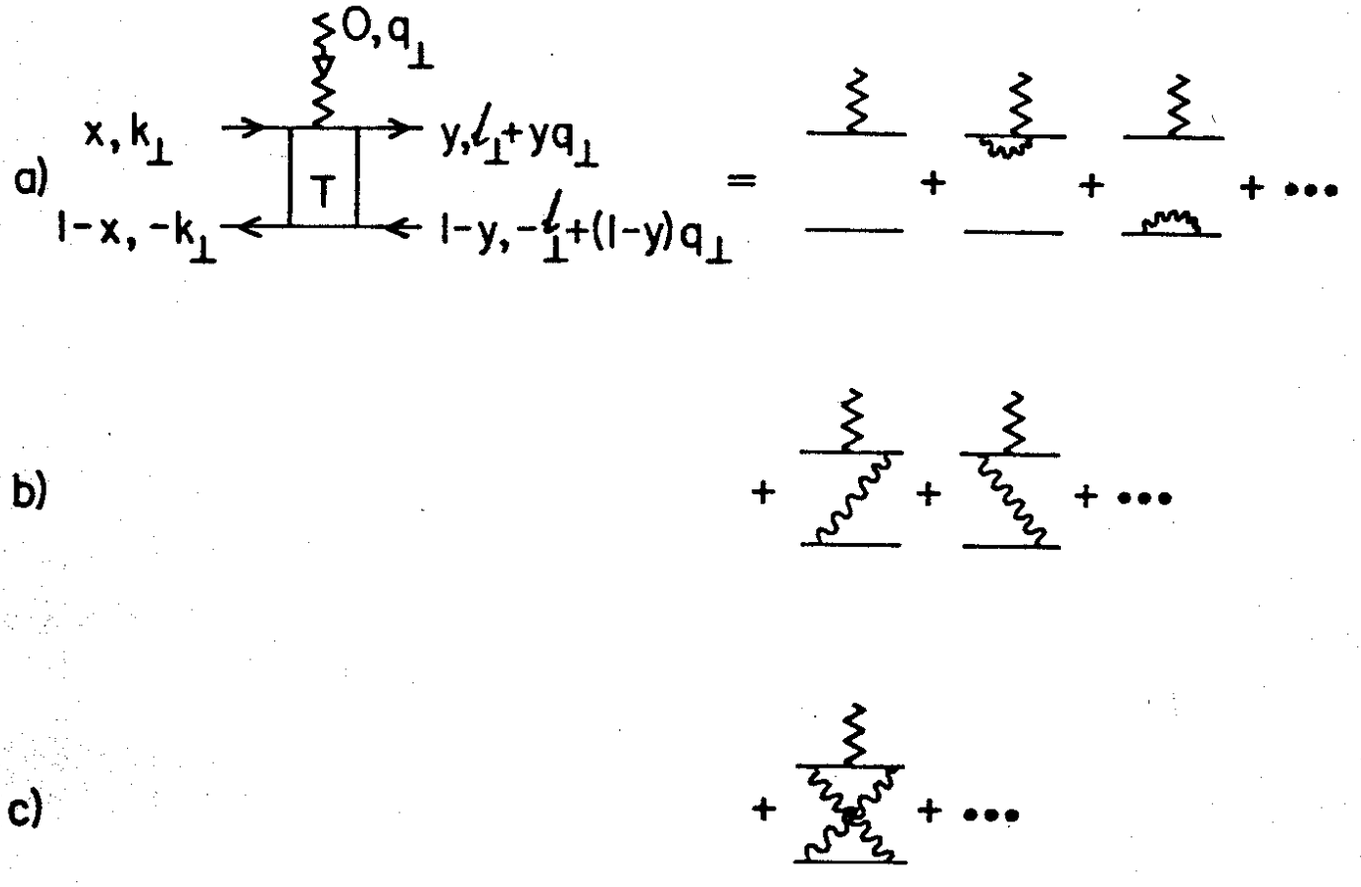

FIG. 11

0771281

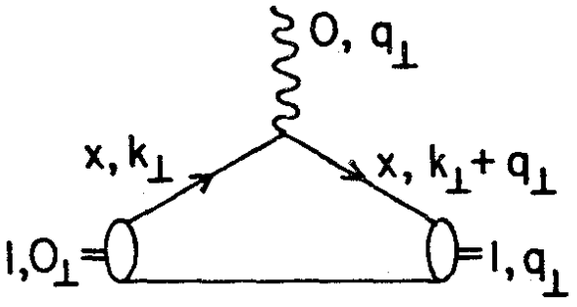

FIG. 12

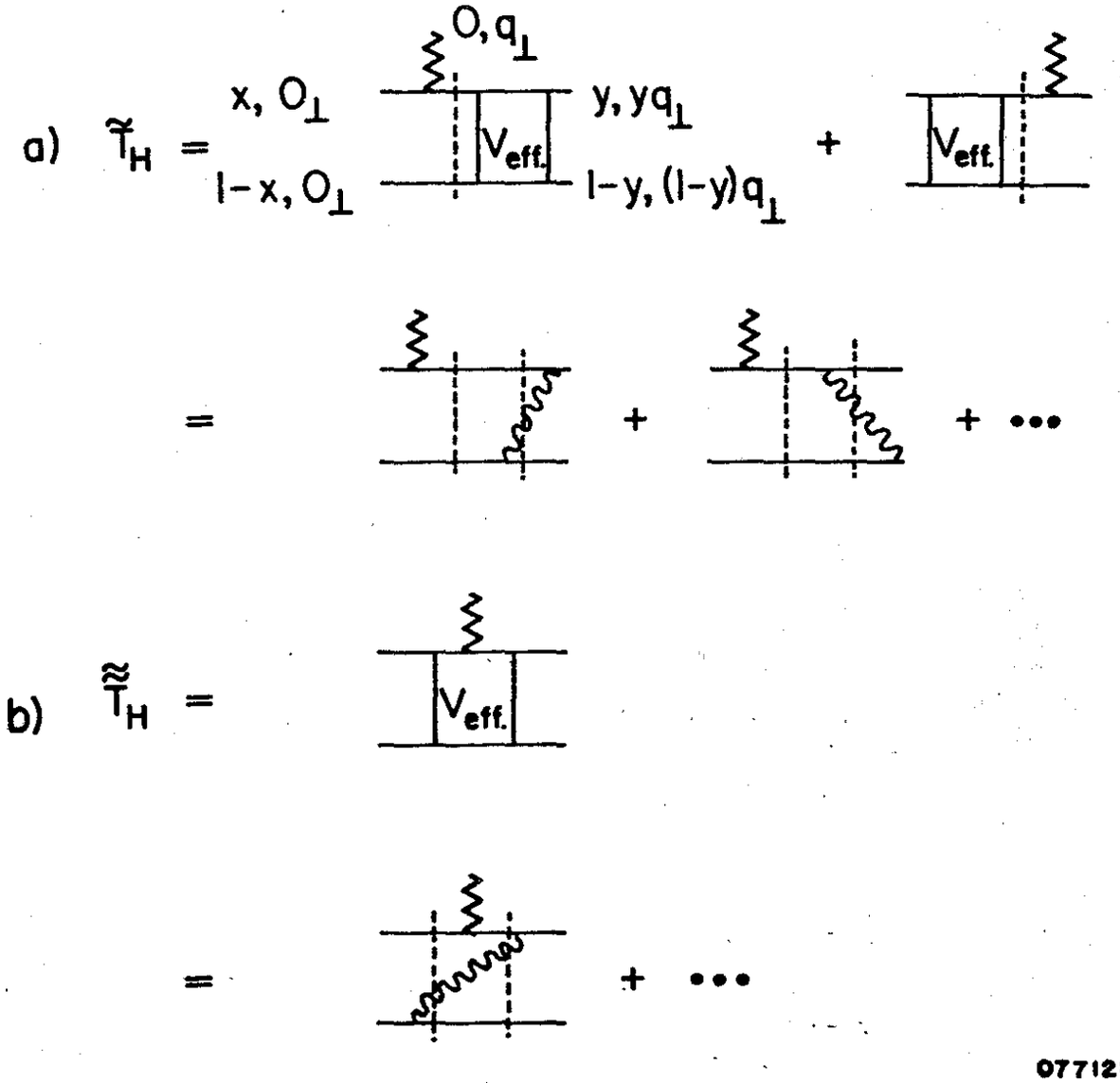

0771281

FIG. 13

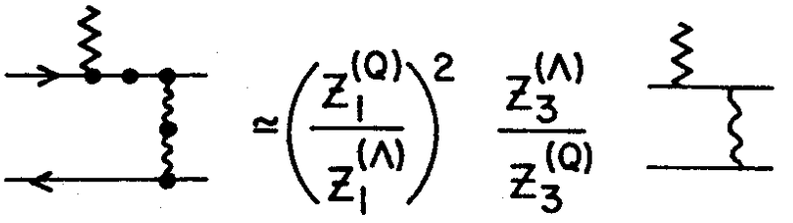

FIG. 14

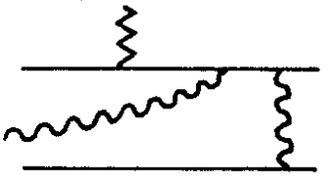

FIG. 15

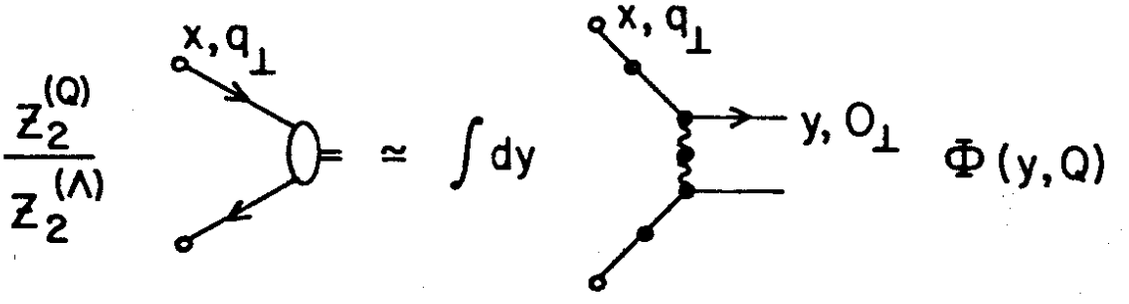

FIG. 16

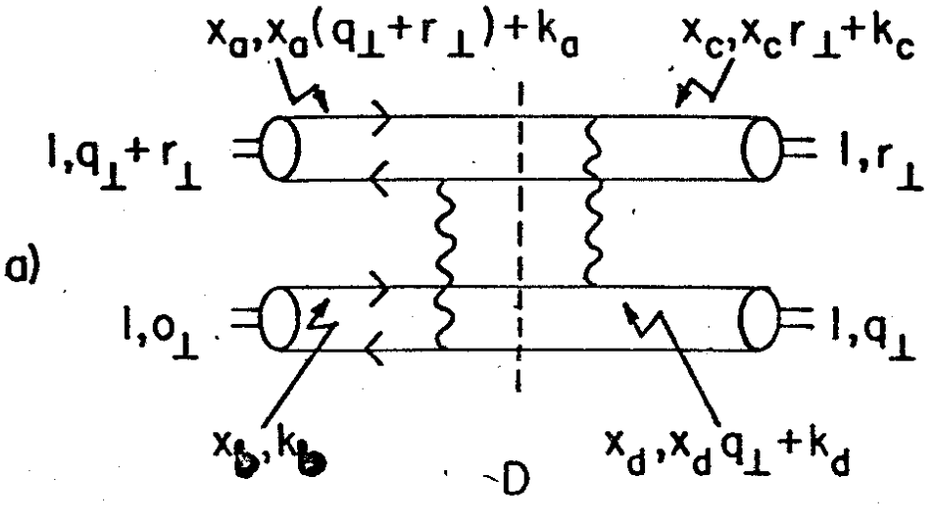
$x_a, x_a(q_\perp + r_\perp) + k_a$
$x_c, x_c r_\perp + k_c$
$1, q_\perp + r_\perp$
$1, r_\perp$
a)
$1, o_\perp$
$1, q_\perp$
x_b, k_b
D
$x_d, x_d q_\perp + k_d$

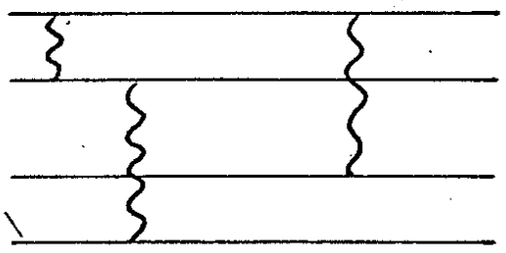
b)

FIG.17

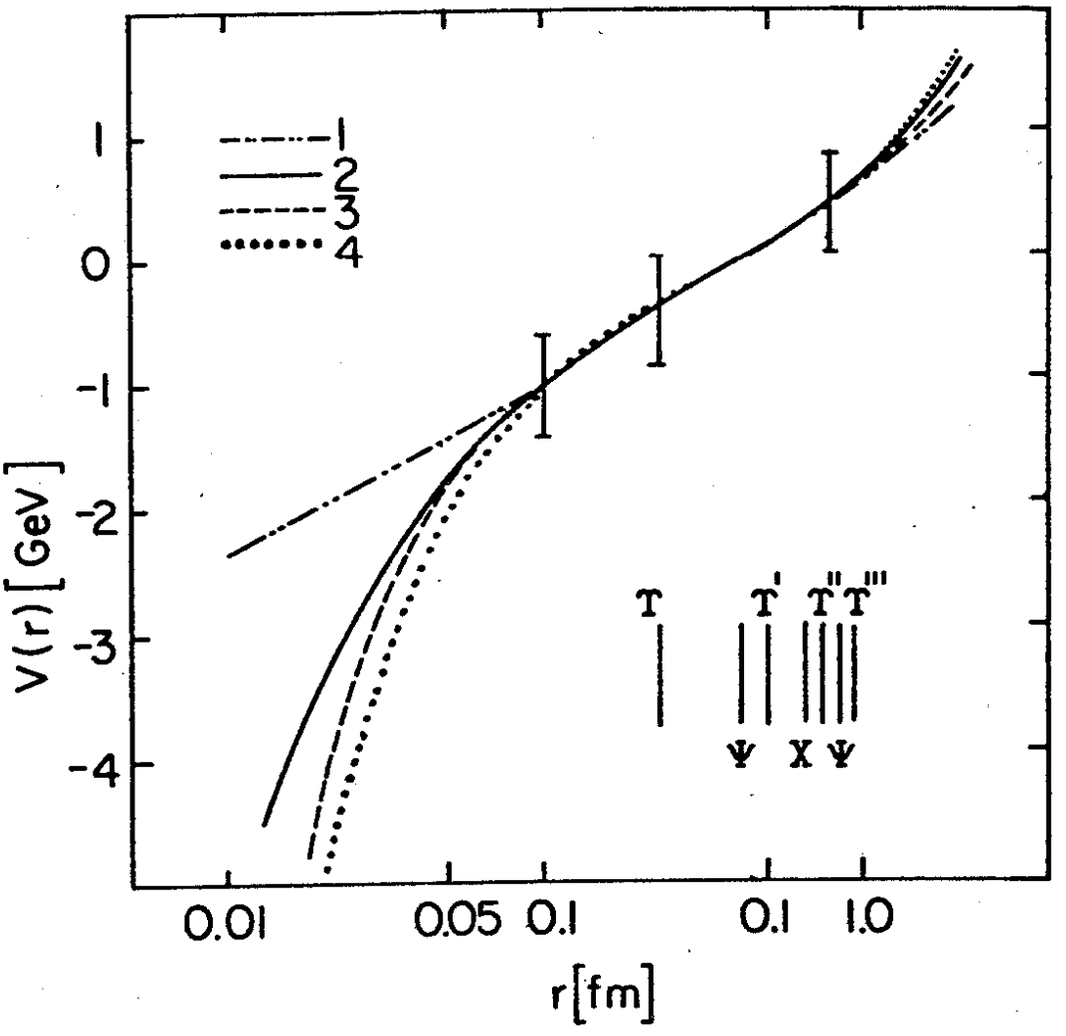

FIG.18

0771281

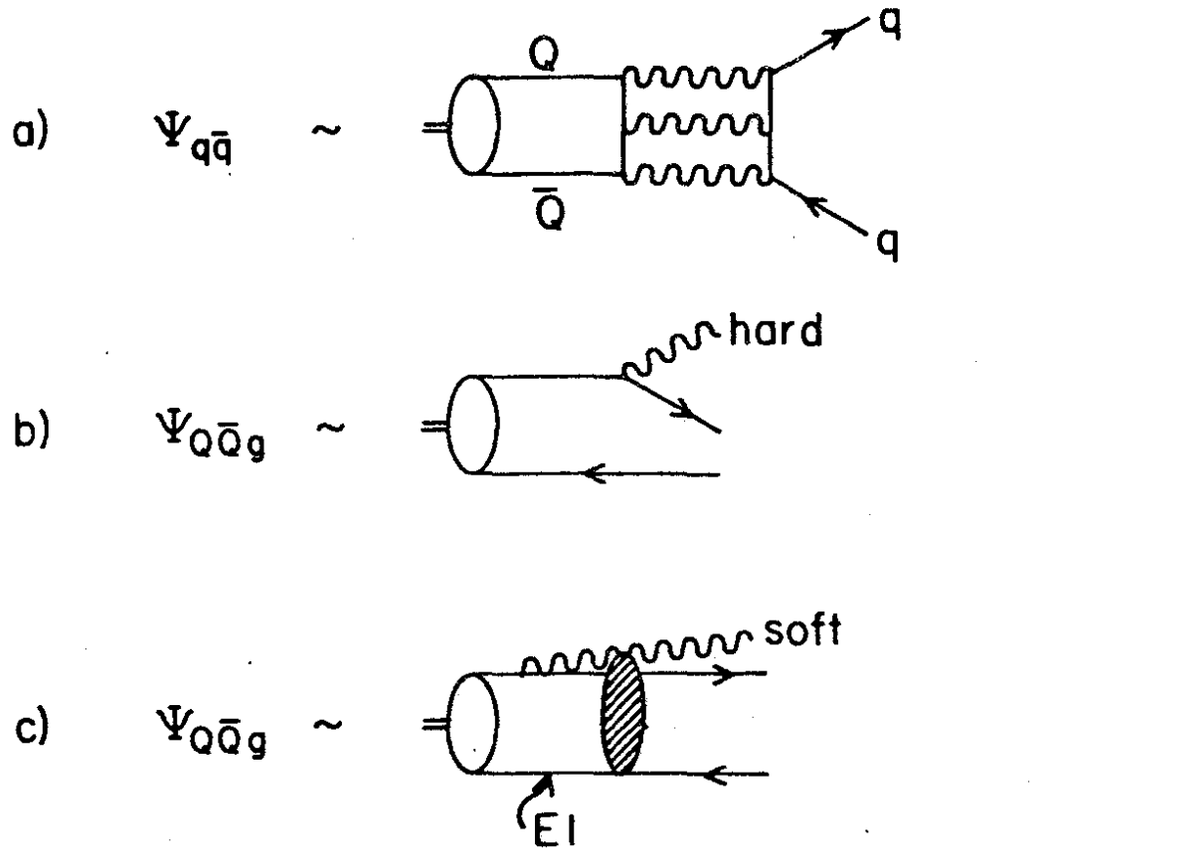

FIG. 19

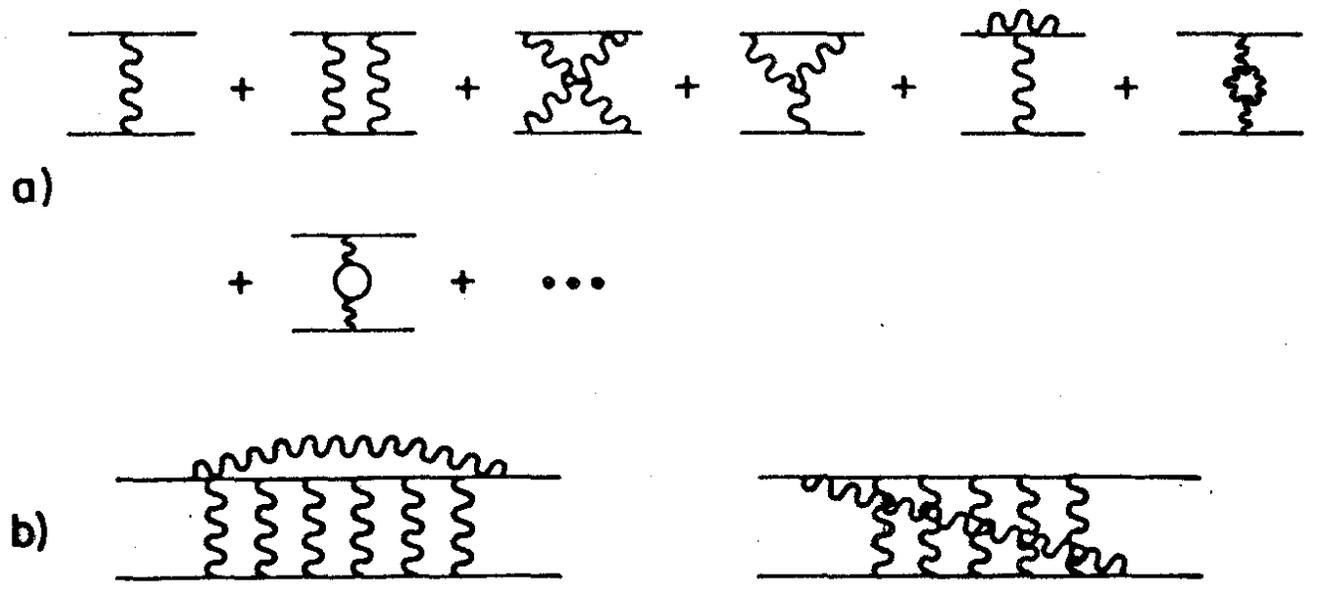

FIG. 20

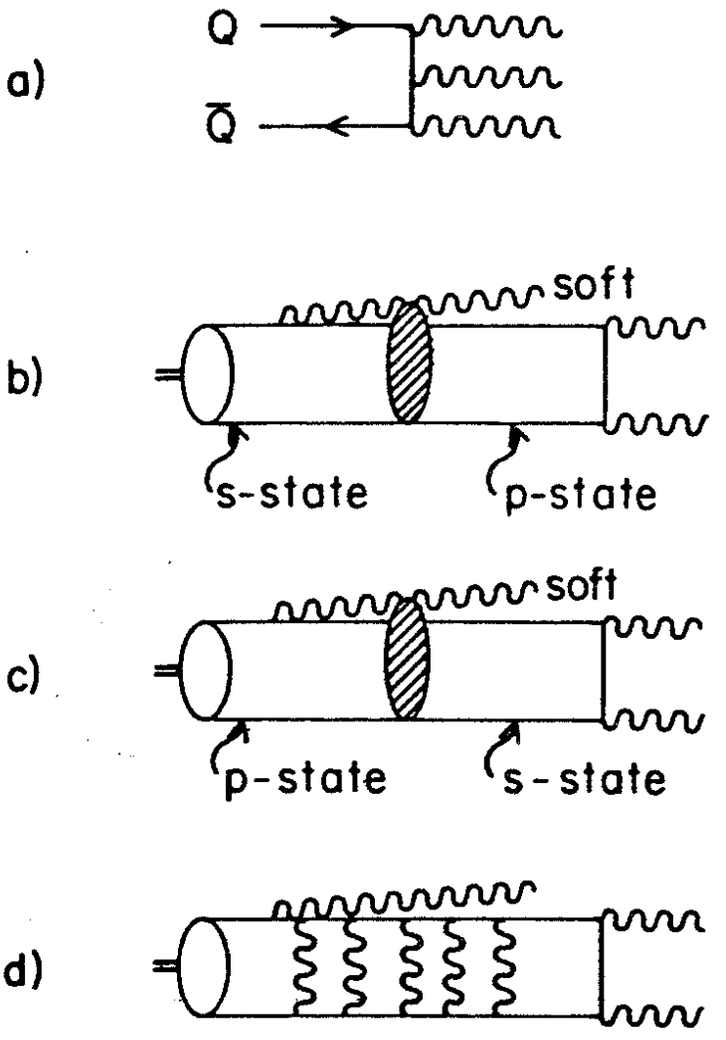

FIG. 21

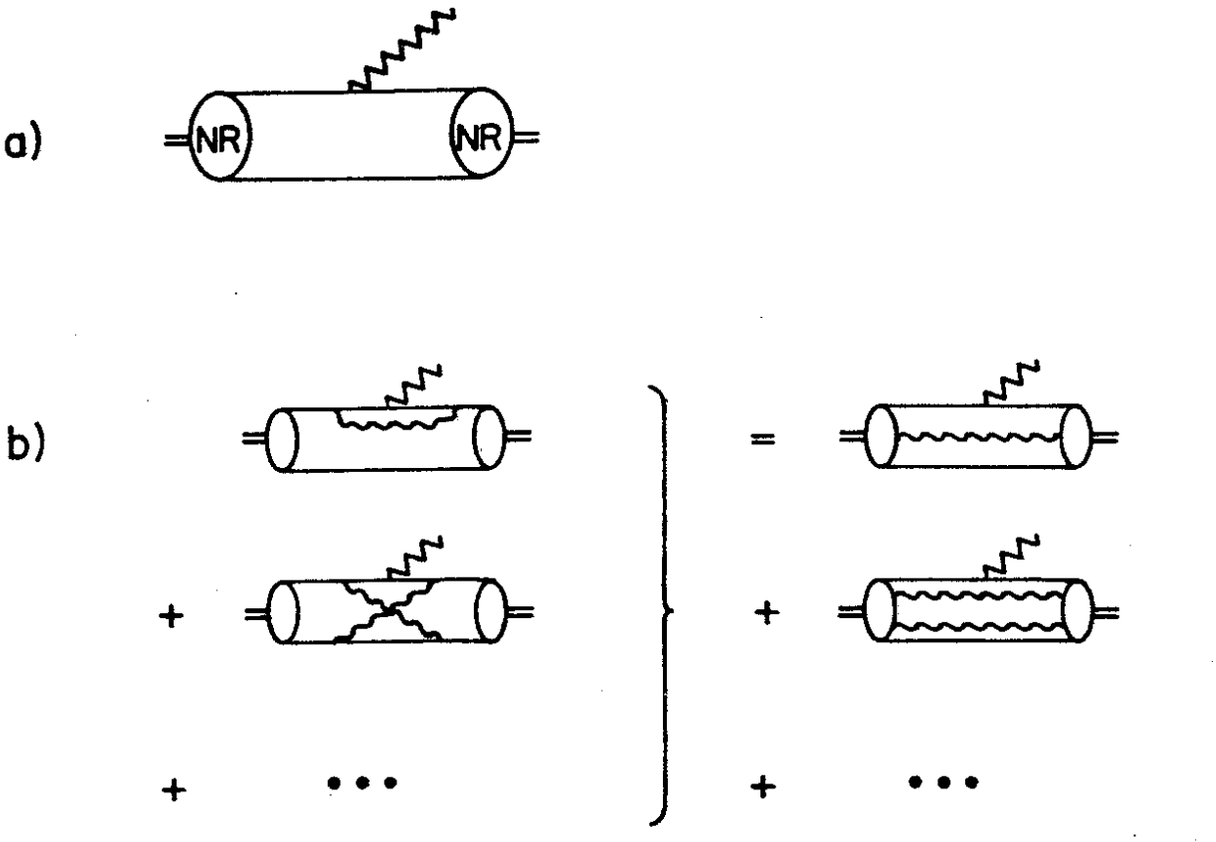

FIG. 22

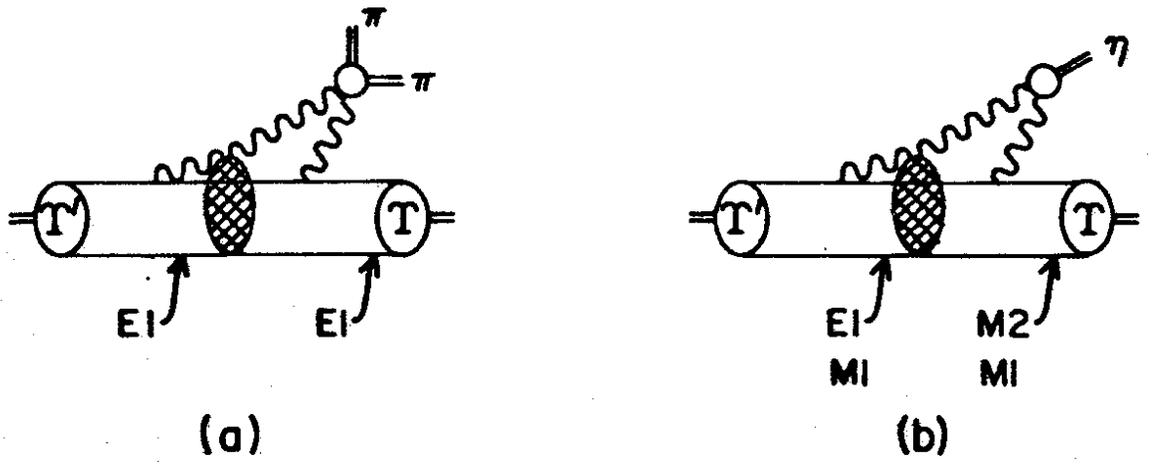

FIG. 23

0771281

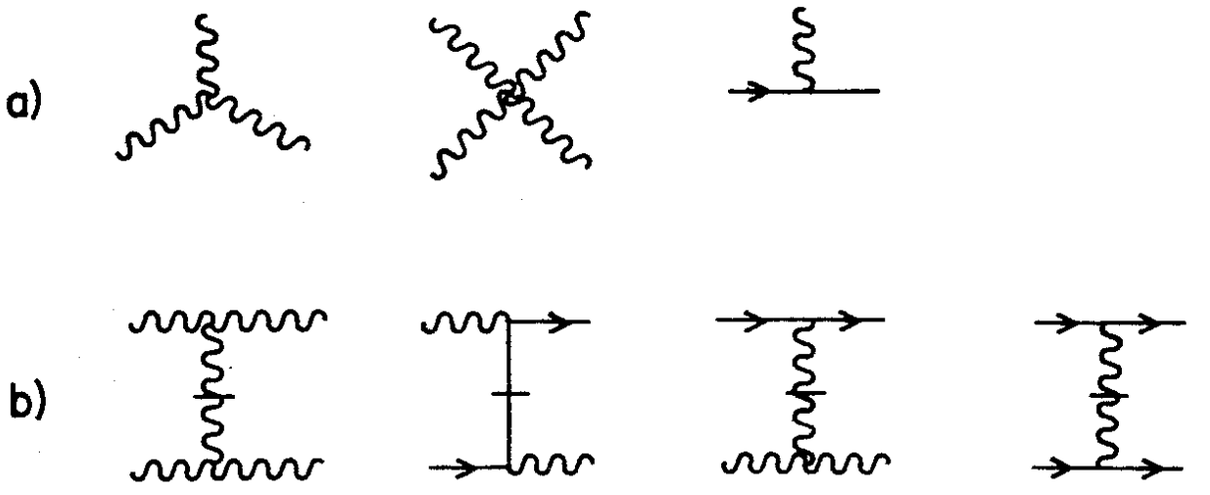

FIG. 24

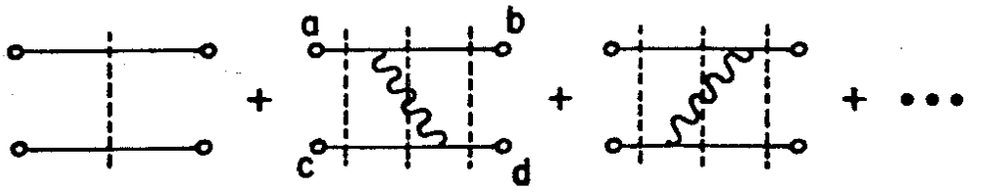

FIG. 25

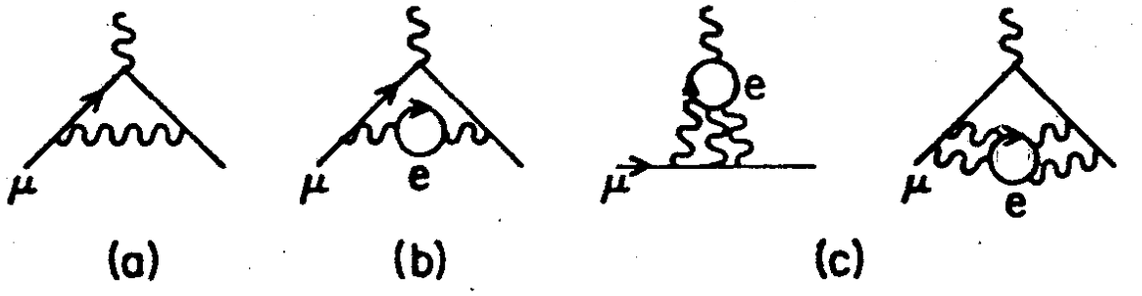

FIG. 27

	Vertex Factor	Color Factor
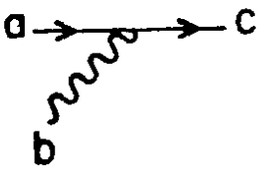	$g\,\bar{u}(c)\,\not{\epsilon}_b\,u(a)$	T^b
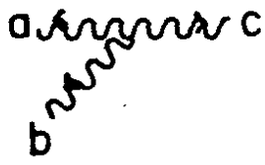	$g\{(p_a-p_b)\cdot\epsilon_c^*\;\epsilon_a\cdot\epsilon_b$ + cyclic permutations$\}$	iC^{abc}
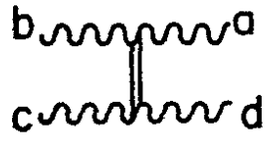	$g^2\{\epsilon_b\cdot\epsilon_c\;\epsilon_a^*\cdot\epsilon_d^*+\epsilon_a^*\cdot\epsilon_c\epsilon_b\cdot\epsilon_d^*\}$	$iC^{abe}iC^{cde}$
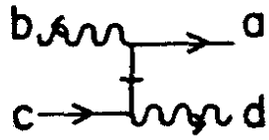	$g^2\,\bar{u}(a)\,\not{\epsilon}_b\,\frac{\gamma^+}{2(p_c^+-p_d^+)}\,\not{\epsilon}_c^*\,U$	T^bT^d
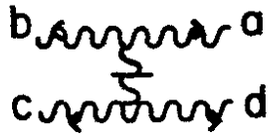	$g^2\,\epsilon_a^*\cdot\epsilon_b\,\frac{(p_a^+-p_b^+)(p_c^+-p_d^+)}{(p_c^++p_b^+)^2}\,\epsilon_d^*\cdot\epsilon_c$	$iC^{abe}iC^{cde}$
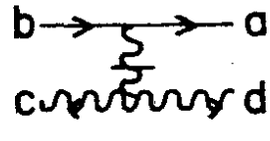	$g^2\,\bar{u}(a)\gamma^+u(b)\;\frac{(p_c^+-p_d^+)}{(p_c^++p_d^+)^2}\,\epsilon_d^*\cdot\epsilon_c$	$iC^{cde}\,T^e$
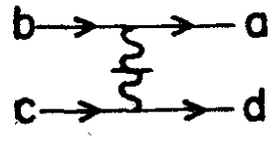	$g^2\,\frac{\bar{u}(a)\gamma^+u(b)\;\bar{u}(d)\;\gamma^+u(c)}{(p_c^+-p_d^+)^2}\;T^e\,T^e$	

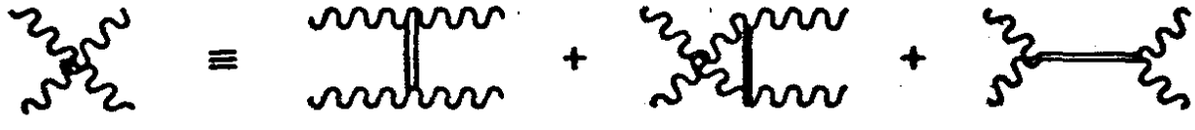

FIG. 26

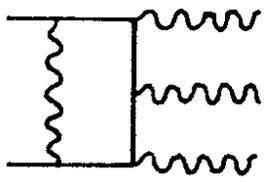

FIG. 28